© 2014. Published by The Company of Biologists Ltd | Development (2014) 141, 3649-3661 doi:10.1242/dev.111880

RESEARCH ARTICLE

EphA4-dependent Brachyury expression is required for dorsal mesoderm involution in the *Xenopus* gastrula

Sevan Evren, Jason W. H. Wen, Olivia Luu, Erich W. Damm, Martina Nagel and Rudolf Winklbauer*

ABSTRACT

Xenopus provides a well-studied model of vertebrate gastrulation, but a central feature, the movement of the mesoderm to the interior of the embryo, has received little attention. Here, we analyze mesoderm involution at the *Xenopus* dorsal blastopore lip. We show that a phase of rapid involution – peak involution – is intimately linked to an early stage of convergent extension, which involves differential cell migration in the prechordal mesoderm and a new movement of the chordamesoderm, radial convergence. The latter process depends on *Xenopus* Brachyury, the expression of which at the time of peak involution is controlled by signaling through the ephrin receptor, EphA4, its ligand ephrinB2 and its downstream effector p21-activated kinase. Our findings support a conserved role for Brachyury in blastopore morphogenesis.

KEY WORDS: Gastrulation, *Xenopus*, EphA4, Brachyury, Involution

INTRODUCTION

Moving endoderm and mesoderm from the surface to the interior of the embryo is fundamental to gastrulation. A basic form of germ layer internalization is invagination, but in many vertebrates the process is more complex. In *Xenopus*, a blastopore forms by bottle cell constriction at the vegetal rim of the marginal zone (Hardin and Keller, 1988). Above the blastopore groove, the blastopore lip contains mesoderm and a covering layer of suprablastoporal endoderm. The lip involutes, i.e. it rolls inward to position the mesoderm between ectoderm and the endodermal lining of the archenteron (Fig. 1A,A′) (Keller, 1981). Dorsally, a burst of rapid 'peak involution' is followed by slow involution during constriction of the ring-shaped blastopore, which eventually closes below the vegetal endoderm (Keller and Danilchik, 1988; Winklbauer and Schurfeld, 1999; Ewald et al., 2004). Internalization at the blastopore is complemented by additional processes (see Fig. 11A). The vegetal cell mass surges inward during vegetal rotation, aiding in the internalization of the sub-blastoporal endoderm (Winklbauer and Schurfeld, 1999). Animally, the epibolic spreading of the ectodermal blastocoel roof (BCR) compensates for the vegetal displacement of the constricting blastopore (Keller, 1980).

Despite its major role in amphibian gastrulation, involution has not yet been analyzed comprehensively. The notion that bottle cells tug the mesoderm in (Rhumbler, 1902) has been refuted for *Xenopus*: internalization proceeds even after excision of the bottle cells, and transplantation experiments identified the mesoderm as driving involution (Keller, 1981). At the ventral blastopore, cell migration through the lip along arc-like trajectories possibly contributes to involution (Ibrahim and Winklbauer, 2001). Dorsally, generation of a hoop stress across the blastopore lip by mediolateral cell intercalation has been proposed to promote involution (Keller et al., 1992; Shih and Keller, 1992). Here, we show that radial-animally oriented cell movement is associated with peak involution at the dorsal blastopore. Its execution requires the T-box transcription factor *Xenopus* Brachyury (Xbra) (Smith et al., 1991), the expression of which is controlled by the tyrosine kinase receptor EphA4 (Pagliaccio/Sek-1) (Winning and Sargent, 1994) and its effector, p21-activated kinase 1 (Pak1) (Bisson et al., 2007).

In the *Xenopus* gastrula, several Eph receptors and ephrin ligands are expressed and required for ectoderm-mesoderm boundary maintenance (Rohani et al., 2011; Park et al., 2011; Hwang et al., 2013) and axis specification (Tanaka et al., 1998). EphA4 is expressed in the mesoderm (Winning and Sargent, 1994) to contribute to boundary maintenance (Park et al., 2011). Its ectopic expression in ectoderm diminishes cell adhesion (Winning et al., 1996, 2001) through Nck-mediated recruitment of Pak1, which in turn prevents activation of RhoA (Winning et al., 2002; Bisson et al., 2007). Activation of Paks by recruitment to receptor tyrosine kinases is common (Lu et al., 1997), and Paks are prominently involved in regulating the cytoskeleton, but also in transcriptional control (Bokoch, 2003; Hofmann et al., 2004). In the *Xenopus* embryo, Pak1 is ubiquitously expressed (Islam et al., 2000) and regulates mesoderm cell migration (Nagel et al., 2009).

Expression of Xbra is controlled by mesoderm-inducing factors of the TGF-β and FGF families, respectively (Smith et al., 1991; Hemmati-Brivanlou and Melton, 1992; Amaya et al., 1993), and by canonical Wnt signaling (Vonica and Gumbiner, 2002; Schohl and Fagotto, 2003). We show that during a short period preceding peak involution, Xbra expression is EphA4-dependent. Xbra has previously been implicated in the specification of posterior mesoderm, prevention of apoptosis, notochord differentiation and convergent extension movements (Smith et al., 1991; Cunliffe and Smith, 1992; Conlon et al., 1996; Conlon and Smith, 1999). We found that during the EphA4-dependent phase Xbra is required for the involution of the dorsal mesoderm.

RESULTS

Autonomous region-specific internalization movements at the dorsal blastopore lip

In *Xenopus*, dorsal mesoderm internalization leads to an S-shaped folding of the blastocoel wall as the marginal zone bends upwards between the neural ectoderm and the vegetal cell mass (Fig. 1A,A′). This folding is an autonomous process. When a sheet of tissue consisting of the epithelial layer and underlying deep cells is explanted at stage 10, it first compacts and the blastopore groove deepens (Fig. 1B). After 2.5 h, at stage 11, the characteristic S-shaped folding pattern with its two inflection points, the tip of the archenteron and the lower end of the blastopore lip, is reproduced (Fig. 1B′). If the lower part of the explant is isolated, consisting of vegetal mass and marginal

Department of Cell and Systems Biology, University of Toronto, 25 Harbord Street, Toronto, Ontario, Canada M5S 3G5.

*Author for correspondence (r.winklbauer@utoronto.ca)

Received 24 April 2014; Accepted 27 July 2014

Development (2014) 141, 3649-3661 doi:10.1242/dev.111880

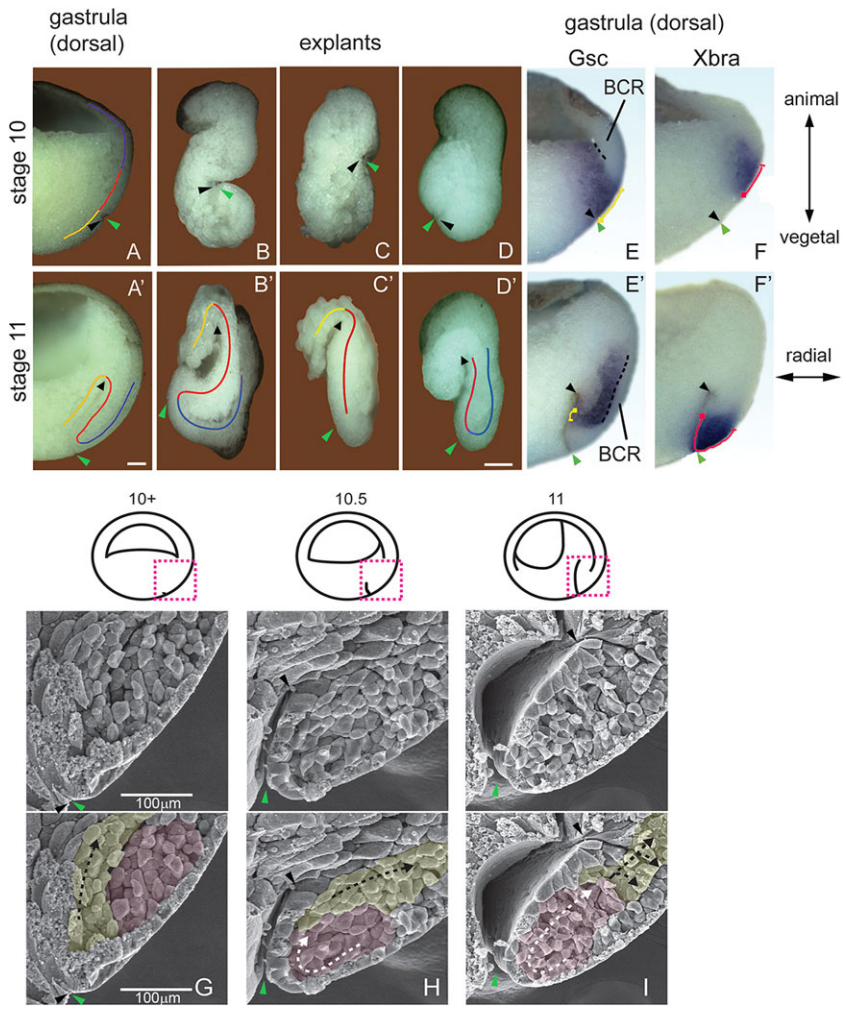

Fig. 1. Internalization at the dorsal blastopore. (A-D′) Tissue folding. The peripheral layers of an initial gastrula (A) (prospective endoderm, mesoderm and ectoderm; yellow, red and blue sections of line, respectively) become folded by the mid-gastrula stage (A′). Explants of whole dorsal region (B), of endoderm and mesoderm (C) and of mesoderm and ectoderm (D) after one hour of excision at stage 10, and after autonomous folding, at stage 11 (B′-D′). (E-F′) Mesoderm regions identified by *in situ* hybridization for *Gsc* (E,E′) and *Xbra* (F,F′) at stages 10 (E,F) and 11 (E′,F′). Yellow line, Gsc domain; red line, Xbra domain. Axes indicated by double arrows. (G-I) SEM pictures of lip. Bottom row, regions: red, Xbra domain; yellow, Gsc domain. Black arrowheads, position of bottle cells; green arrowheads, blastopore. Scale bars: 100 µm. BCR, ectodermal blastocoel roof.

zone, it folds around the blastopore (Fig. 1C,C′). Similarly, an isolated upper part comprising marginal zone and BCR (a lip-BCR explant) folds back on itself with mesoderm and BCR spreading onto each other (Fig. 1D,D′), reproducing involution *in vitro*.

To relate involution to mesoderm regions, expression of the prechordal mesoderm marker Gsc and the chordamesoderm marker Xbra (Winklbauer and Schurfeld, 1999) were visualized (Fig. 1E-F′). Gsc is initially expressed in an arc extending from the lower part of the blastopore lip to the blastocoel floor, separating the Xbra domain from the vegetal cell mass (Fig. 1E). In the mid-gastrula, this region has become fully internalized to spread and extend animally on the BCR. Posteriorly it remains in contact with the internalized epithelial suprablastoporal endoderm (Fig. 1E′). The Xbra domain is first located animally to the Gsc domain (Fig. 1F). After peak involution, its central part forms the tip of the blastopore lip (Fig. 1F′), as if the domain had been bent inward. This identifies the center of the Xbra domain as the lower inflection point in the S-shaped folding pattern of the marginal zone, the upper one being at the site of the bottle cells.

Two distinct cell populations that correspond to the Gsc and Xbra domains, respectively (Damm and Winklbauer, 2011), can also be discerned in the scanning electron microscope (SEM) (Fig. 1G-I). As early as stage 10+, an arc of elongated cells, the Gsc domain, stretches from the epithelial layer near the bottle cells to the BCR. It surrounds, and is clearly separated from, a core of cells in the center of the lip, the Xbra domain (Fig. 1G). By the onset of peak involution, the epithelial layer has moved inward, generating a short archenteron. Adjacent deep cells are elongated in parallel to the epithelium, consistent with inward migration of cells in the Gsc domain (Fig. 1H). When internalized Gsc cells reach positions opposite the BCR, they orient towards it (Fig. 1I) (Damm and Winklbauer, 2011). In the Xbra domain, cell shapes and orientations are irregular when viewed in the sagittal plane (Fig. 1G-I).

Convergent extension is an integral part of dorsal involution

How lip-BCR explants (Fig. 1D,D′) fold is revealed in time-lapse recordings (Fig. 2A-F; supplementary material Movie 1). Explants round up, while at the vegetal side a blastopore lip forms (Fig. 2A). With the onset of peak involution (stage 10.5), two movements can be distinguished (Fig. 2B-F). First, as the marginal zone spreads onto the BCR, it moves animally while tissue is continually added behind by rolling over the lip, constituting involution. Second, the advancing post-involution tissue converges towards the midline and elongates (Fig. 2C-F; supplementary material Movie 1). Notably, much of this convergent extension involves the Gsc-expressing prechordal mesoderm (Fig. 1E,E′), which occupies the region behind the bottle cells in lip-BCR explants (Fig. 2G) and spreads on the BCR in the course of involution (Fig. 2G′). As in the embryo, the Xbra-expressing chordamesoderm follows behind and bends to form the tip of the blastopore lip in explants (Fig. 2H,H′).

Convergent extension has been studied in open-faced Keller explants, lip-BCR explants that are prevented from involution by

Development (2014) 141, 3649-3661 doi:10.1242/dev.111880

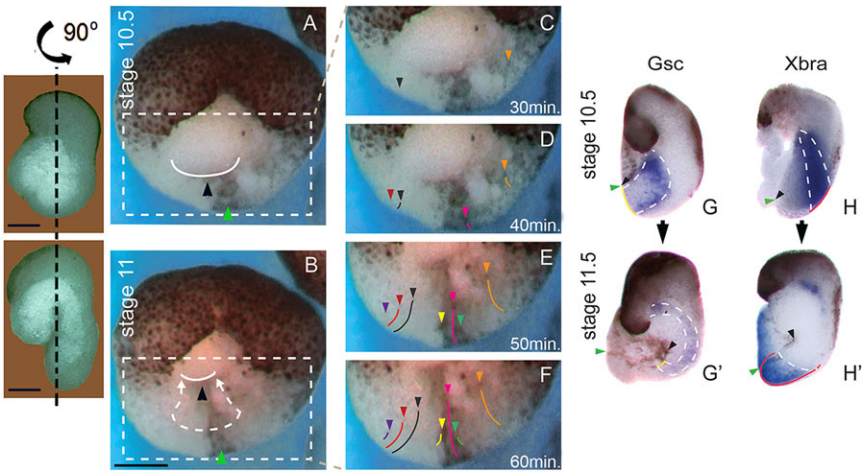

Fig. 2. Lip-BCR explants. (A,B) Frames from time-lapse recording 30 min (A) and 60 min (B) after explantation, viewed from inside the embryo (left, respective sagittal section views of fixed explants, for orientation). Animal to the top, green arrowhead, tip of lip; black arrowhead, bottle cell position. (C-F) Higher magnification of squares in A,B. Arrowheads and lines indicate pathways of landmarks. Sequential appearance of landmarks indicates involution, pathways converge towards midline. (G-H′) Mesoderm regions identified by Gsc and Xbra expression in explants. Arrowheads, red and yellow lines as in Fig. 1E,F. Animal to the top, dorsal to the right. Scale bars: 100 µm.

applying a coverslip (Wilson and Keller, 1991) (Fig. 3E). We confirmed the early onset of cell intercalation in the Gsc domain at the vegetal end of such explants (Fig. 3A,D; supplementary material Movie 2). Cells are elongated and show strong anteriorly directed (towards the former vegetal edge) migration, which is absent from the putative Xbra domain (Fig. 3B,D). Such a difference in motility between the two regions is also expressed in isolated cells (Kwan and Kirschner, 2003).

Within the migratory domain itself, more anterior cells move faster than more posterior cells (Fig. 3D), probably reflecting differences in migration velocities between 'inner' and 'outer' lanes in the lip during internalization (Fig. 3E), which are also evident during ventral involution (Ibrahim and Winklbauer, 2001). The velocity differences lead to the exposure of deep cells at gaps between cells that move apart anteroposteriorly (Fig. 3B,C), a process previously described as directional radial intercalation, the insertion of cells between anterior and posterior neighbors that leads to tissue elongation (Wilson and Keller, 1991; Yin et al., 2008). Moreover, cell rows also converge and merge laterally (Fig. 3B). Thus, differential migration – the directional migration of cells at spatially graded velocities – underlies the convergent extension of the Gsc domain.

Differential migration in the Gsc domain and radial convergence of the Xbra domain are autonomous processes of involution

Involution of the lip mesoderm is independent of the BCR. Lip explants without BCR – lip-only explants – elongated asymmetrically on their vegetal side, and a pointed tip formed (Fig. 4A,A′,D). The increase in cross-sectional area most likely reflects convergence (not

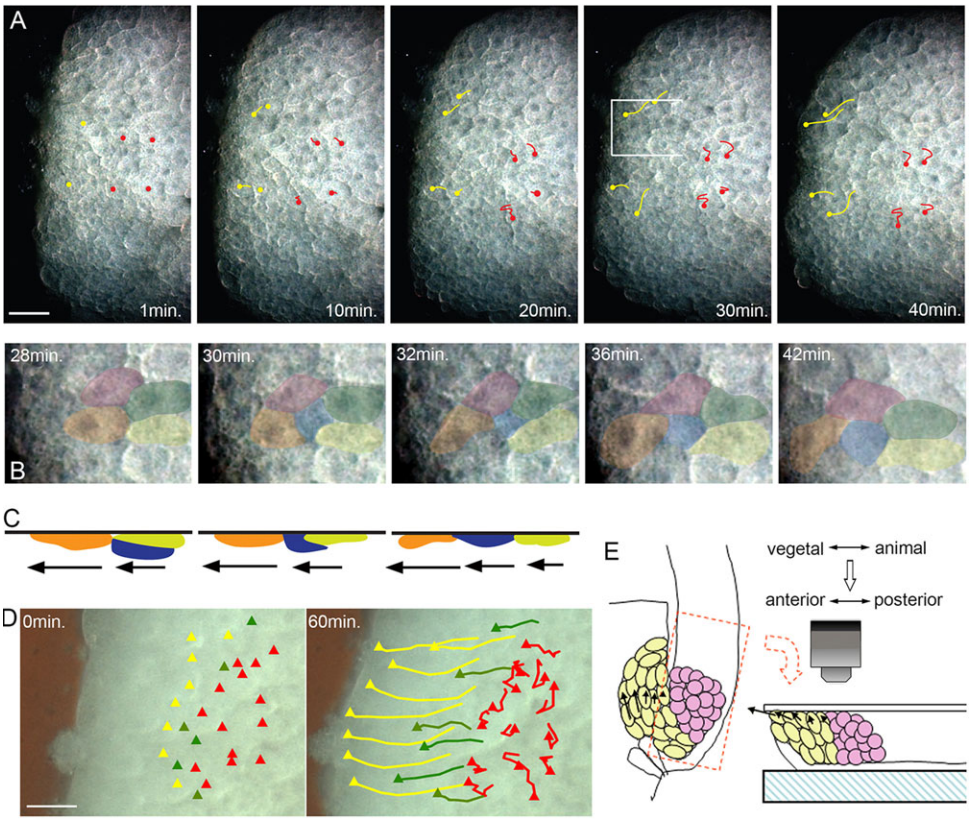

Fig. 3. Open-faced lip-BCR explants. (A) Cell movements in early gastrula explant. Cells at anterior (former vegetal) edge (left) migrate anteriorly (yellow arrows), narrowing and extending the lip tissue. Posterior cells show minor movement (red arrows). (B) Higher magnification of region in A (white rectangle), cell (blue) appears between cells moving apart, and lateral cell neighbors (red, orange) become anteroposterior neighbors. (C) Intercalation by differential migration. (D) Decreasing cell velocities from anterior (yellow) to posterior (green, red). (E) Interpretative scheme. Yellow, Gsc domain; red, Xbra domain. Explant (dashed rectangle) is secured under coverslip. Arrow lengths indicate velocities: long, outer lanes; short, inner lanes through lip. Vegetal-animal axis becomes anterior-posterior axis after involution. Scale bars: 100 µm.

Development (2014) 141, 3649-3661 doi:10.1242/dev.111880

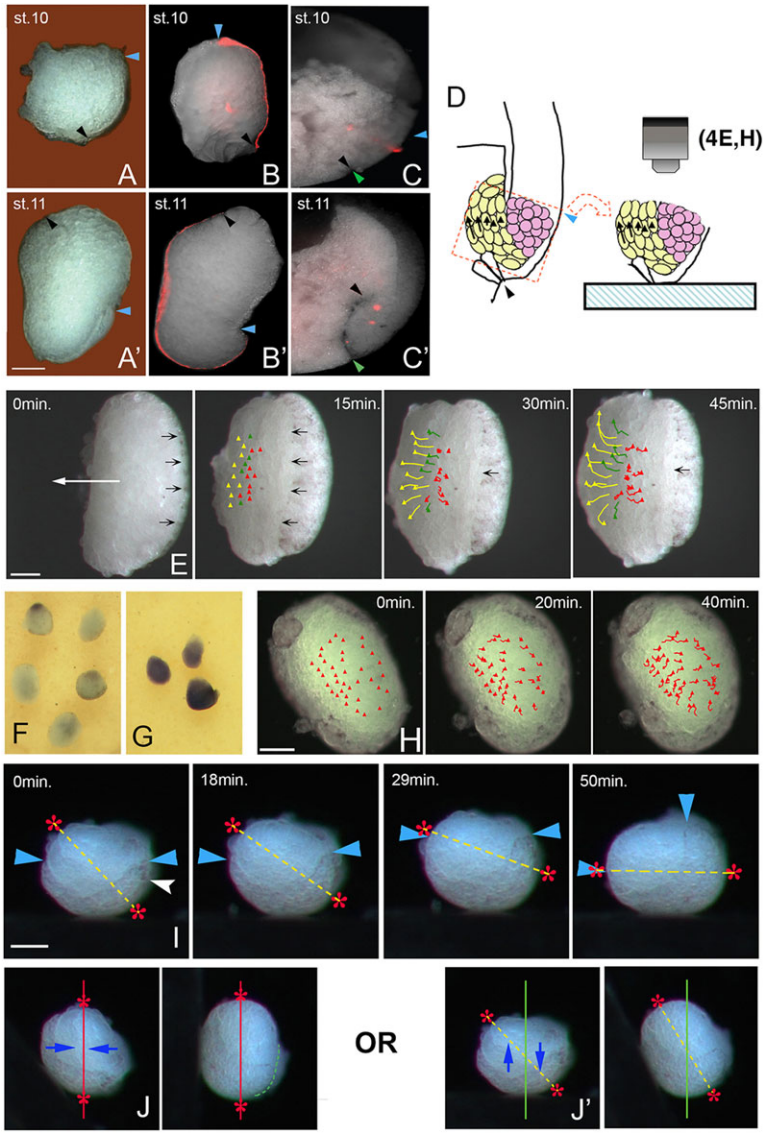

Fig. 4. Lip-only explants. (A-B′) Lip explants without BCR, sagittally fractured. Explants at indirect illumination (A,A′) or with biotinylated/TRITC antibody-labeled surface (B,B′) after explantation (A,B) and 2.5 h later (A′,B′). (C,C′) DiI-labeled line in dorsal lip directly after labeling (C) and after peak involution (C′). Black arrowheads, bottle cell position; green arrowheads, blastopore; blue arrowheads, border between lip and BCR. (D) Schematic of explants as in Fig. 3. (E) Time-lapse recording of lip-only explant. View of cut surface (see D), position of bottle cells to the left. Massive movement to the left makes explant tip over (white arrow in first frame), brings epithelial layer into view (black arrows). Left-to-right gradient of velocities (yellow, green arrows) on left (Gsc domain), random movement (red arrows) on right side (Xbra domain). (F-J′) Xbra domain explants made at stage 10.5. *In situ* hybridization for *Gsc* (F) or *Xbra* (G), explants fixed, fractioned sagittally 45 min after excision. (H) Time-lapse film of Xbra domain, same view as in E, random cell movements (red arrows), long axis corresponds to lateral extension of lip. (I) Xbra domain filmed in side view in 45° mirror. Landmarks (asterisks) indicating axis of elongation (dashed yellow line), blue arrowheads, upper margins of epithelium; white arrowhead, pigmentation indicates pre-involution side of explant. (J,J′) Interpretation of movement in I: narrowing towards red axis (J) or shear movement along green axis (J′) both lead to radial convergence. Scale bars: 100 µm.

shown). Surface labeling indicated that the epithelial layer wrapped around the lip tissue (Fig. 4B,B′). In time-lapse recordings of lip-only explants, cells of the putative Gsc domain moved over each other towards the bottle cell side until the explant tipped over (Fig. 4E; supplementary material Movie 3). As migration continued (Fig. 4E), deeper cells became exposed as cells above them moved apart (supplementary material Movie 3). In the putative Xbra domain, no distinct movement occurred (Fig. 4E).

The migration of Gsc cells is not necessary for the shape change of the Xbra domain. Lip explants without Gsc domain, i.e. isolated Xbra regions, elongated (Fig. 4F,G), but no distinct migration occurred at the cut surface, as expected from the absence of Gsc cells (Fig. 4H; supplementary material Movie 4; compare with Fig. 4E). When filmed in side view (corresponding to sagittally fractured explants), Xbra domain explants narrowed asymmetrically, becoming longer at the post-involution side and tipping over in the process (Fig. 4I; supplementary material Movie 5). The eventual long axis projects onto an oblique initial position, and explant deformation can be explained by a movement of cells towards this axis (Fig. 4J), by a shear movement obliquely oriented to the axis (Fig. 4J′) or by a combination of these movements; unfortunately, cell morphology (see Fig. 1G-I) is not informative here. At any rate, the lip narrows radially and elongates asymmetrically, and we will refer to this autonomous shape change as radial convergence. In the embryo, a line of DiI label perpendicular to the surface of the lip (Fig. 4C) was rotated by 90° during peak involution (Fig. 4C′) to run through the pointed end of the lip and in the narrow space between archenteron and BCR, confirming that radial convergence of the lip occurs also in the embryo.

In summary, the isolated blastopore lip is capable of an autonomous shape change, which appears as peak involution. It consists of mediolateral convergence, and of an inward and animally directed movement that rotates, elongates and thins the lip region. It is driven by the radial convergence of the Xbra domain through an unknown cellular mechanism, and by the inward-upward migration of Gsc cells. Together, the movements constitute the first phase of convergent extension (Wilson and Keller, 1991), which is thus intimately linked to involution. We show in the following that peak involution depends on radial convergence, and that this shape change of the Xbra domain requires Xbra function.

EphA4 function is necessary for peak involution

Knocking down EphA4 with morpholino antisense oligonucleotides (EphA4-MO; Park et al., 2011) inhibited archenteron formation

Development (2014) 141, 3649-3661 doi:10.1242/dev.111880

(Fig. 5A,B). Mouse *Epha4* mRNA also reduced archenteron elongation at high doses, but rescued EphA4-MO embryos when co-injected at a low dose (Fig. 5A,B). *Xenopus EphA4* mRNA, which was not recognized by the EphA4-MO, was similarly active (supplementary material Fig. S1A,B). The kinase function of EphA4 is required in this context: a kinase-dead KD-EphA4 construct was unable to rescue EphA4 morphants and acted dominant-negatively when overexpressed alone (supplementary material Fig. S1C,D). Expression of mesodermal markers Gsc and Chordin, mesendodermal Cerberus and neural Sox2 were not affected by EphA4-MO injection, although the location of the mesodermal domains was altered, consistent with an effect on tissue movement, but not cell fate specification (supplementary material Fig. S2).

Defective archenteron formation was due to impaired involution. Folding of lip-BCR explants was attenuated by EphA4-MO, and rescued by co-injection of *EphA4* mRNA (Fig. 5C,E). Moreover, whereas in controls Xbra was expressed at the tip of the lip after involution (Fig. 2H′), it remained in its initial position in explants from EphA4 knockdown embryos (Fig. 5D). Apparently, the bending of the Xbra domain normally associated with peak involution requires EphA4 function.

Pak1 acts downstream of EphA4 during peak involution

Dominant-negative DN-Pak1 also affects archenteron formation (Nagel et al., 2009), and the pattern of Gsc and Xbra expression was consistent with an involution defect (Fig. 6A). As with EphA4-MO (supplementary material Fig. S2), the Gsc domain extended from the non-internalized blastopore animally, suggesting that cells moved normally, but that the archenteron did not follow inward, and the Xbra domain did not bend but remained on the surface of the embryo. Lip-BCR explants from DN-Pak1 embryos did not fold properly, but were rescued by Pak1 (Fig. 6B,C; supplementary material Movie 6), and the characteristic shape changes in lip-only explants were also reversibly inhibited by DN-Pak1 (Fig. 6D,E). Finally, as Pak1 is a possible effector of EphA4 (Bisson et al., 2007), we co-injected EphA4-MO with *Pak1* mRNA. Archenteron formation was restored in embryos at a dose of *Pak1* mRNA that alone inhibited archenteron formation (Fig. 6F,G), and folding of lip-BCR explants was similarly rescued (Fig. 6H,I). This suggests that EphA4 controls involution by signaling through Pak1, although the closely related Pak2 and Pak3 are also expressed in the gastrula (Cau et al., 2000; Souopgui et al., 2002) and could be targeted by DN-Pak1.

EphA4-Pak1 signaling controls Xbra expression

We had noticed that Xbra expression was often, but not always, reduced in EphA4 morphants. Closer examination revealed that EphA4 was required during a narrow time period before peak involution. Xbra is first expressed in the late blastula, but EphA4-MO injection had no effect at this stage (Fig. 7A). Furthermore, expression after peak involution was not affected in embryos (Fig. 7B) or lip explants (Fig. 5D) even though involution was inhibited. However, in the early gastrula, Xbra expression was reduced by EphA4-MO in the embryo (Fig. 7C) and in explants (Fig. 5D). DN-Pak1 similarly inhibited Xbra expression in the early gastrula (Fig. 7D), but not earlier, or after stage 11 (see Fig. 6A).

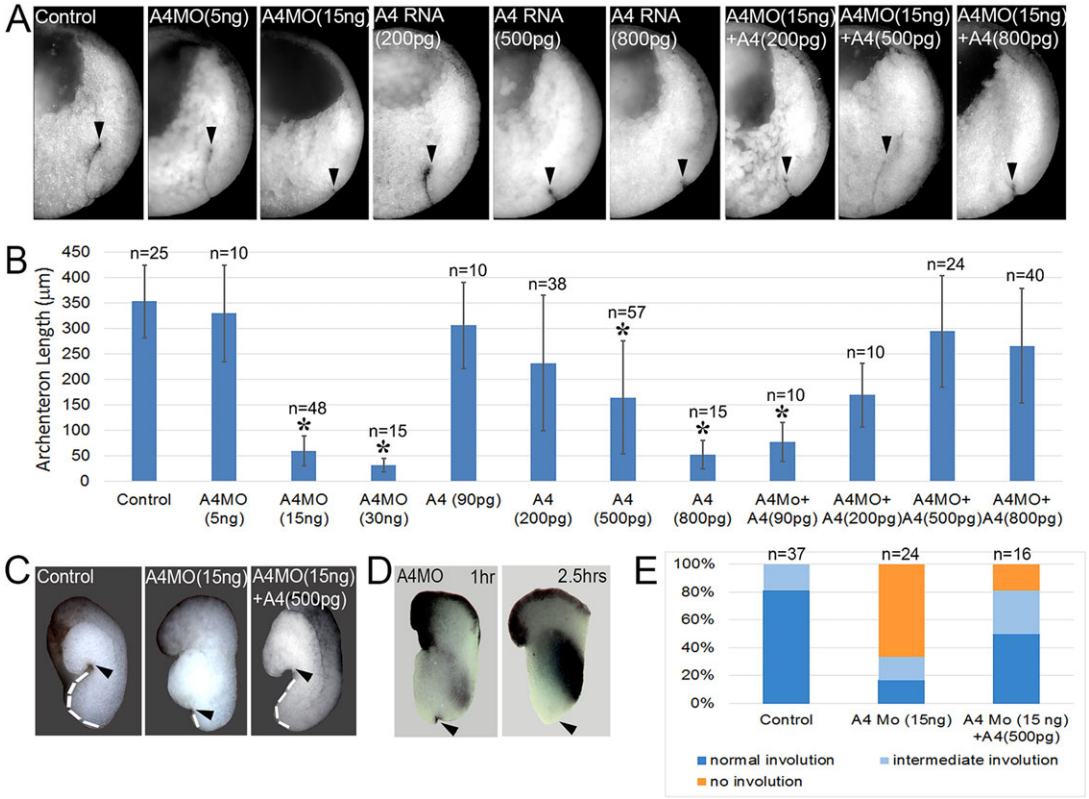

Fig. 5. EphA4 knockdown inhibits peak involution. (A) Embryos fixed and fractured sagittally after peak involution (stage 11) after injection with EphA4-MO and/or *EphA4* mRNA at doses indicated. Arrowheads, position of bottle cells at end of archenteron. (B) Archenteron lengths in experiments shown in A; n, number of embryos; bars indicate s.d.; asterisks indicate significance levels at least $P<0.05$. (C) Lip-BCR explants, sagittal view. Treatments indicated; lengths of involuted surface indicated by dashed line. (D) EphA4-MO-injected lip-BCR explants fixed 1 and 2.5 h after explantation at stage 10+. *In situ* hybridization shows *Xbra* expression. Black arrowheads, position of bottle cells in C,D. (E) Involution defects in lip-BCR explants; n, number of explants.

Development (2014) 141, 3649-3661 doi:10.1242/dev.111880

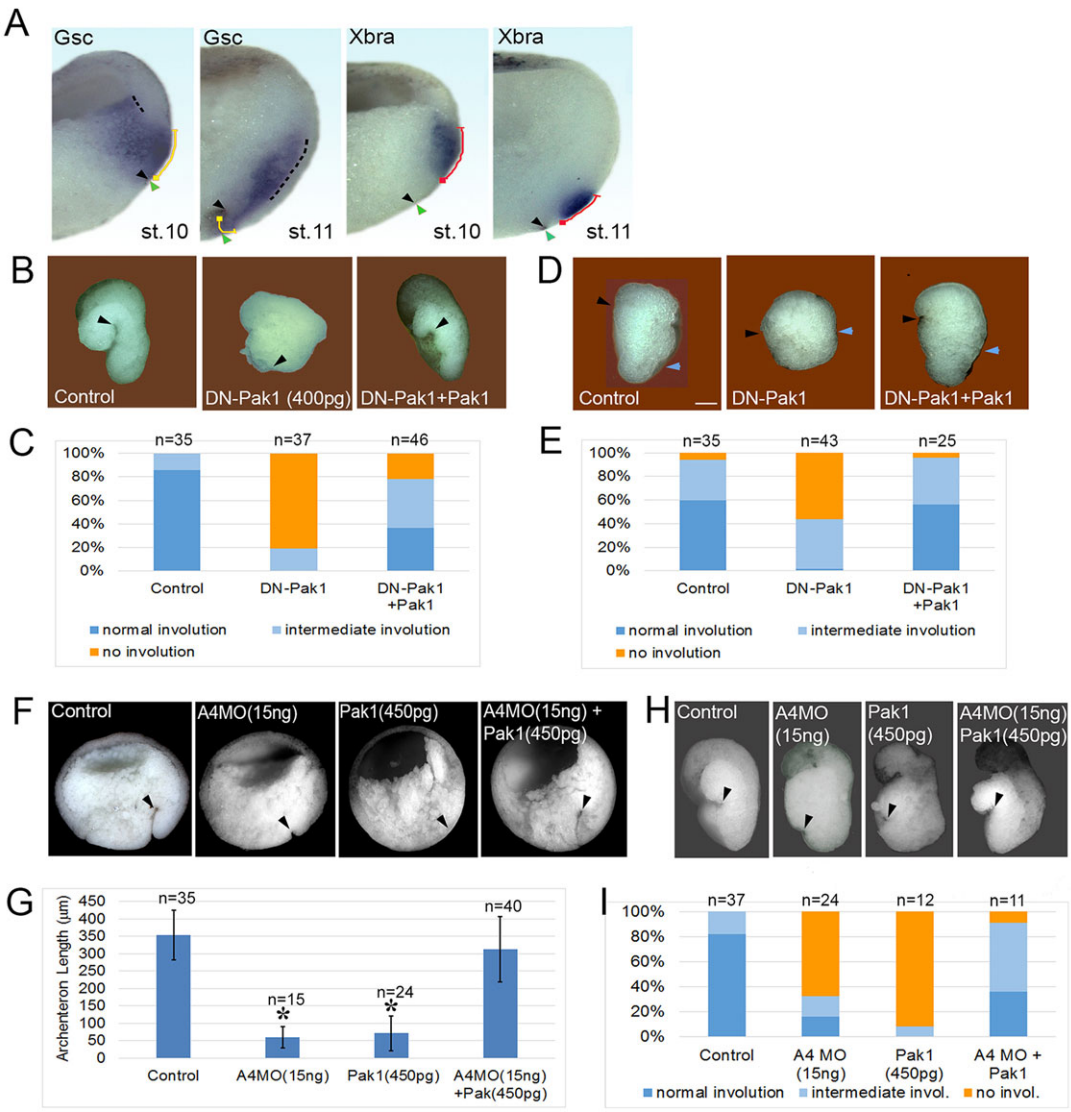

Fig. 6. Pak1 acts downstream of EphA4. (A) *In situ* hybridization for *Gsc* and *Xbra* in DN-Pak1 embryos. Arrowheads, lines as in Fig. 1. (B,C) Pak1 inhibition in lip-BCR explants. (D,E) Pak1 inhibition in lip-only explants. (F) Embryos fractured sagittally after peak involution, rescue of EphA4-MO effect by Pak1. (G) Archenteron lengths in experiments shown in F; n, number of embryos; bars indicate s.d.; asterisks indicate significance levels at least $P<0.05$. (H) Lip-BCR explants. (I) Involution defects in lip-BCR explants; n, number of explants. Black arrowheads, bottle cells positions; green arrowheads, blastopore; blue arrowheads, border between BCR and blastopore lip.

Pak1 mRNA rescued Xbra expression in EphA4 morphants (Fig. 7D), consistent with Pak1 acting downstream of EphA4 to control Xbra expression in the early gastrula.

Pak1 or constitutively active Pak1 (CA-Pak1) (Fig. 7D) did not cause ectopic Xbra expression. However, when Xbra expression was rescued by *EphA4* mRNA or when *EphA4* mRNA alone was injected, additional expression was induced outside the Xbra domain (Fig. 7E). When the injection was targeted to the dorsal marginal zone, *Xbra* transcripts appeared in the anterior mesoderm, whereas animally targeted injection caused expression along the inner surface of the BCR, which was in contact with the mesoderm. Ectopic EphA4-induced Xbra expression was reduced upon co-injection of DN-Pak1, and it also disappeared normally at stage 11 (Fig. 7F), consistent with a transient induction of Xbra by EphA4/Pak1 similar to the endogenous process.

We confirmed that Xbra expression before its EphA4-dependent stage requires FGF signaling (Fletcher and Harland, 2008). Inhibiting the FGF receptor with SU5402 before the onset of zygotic transcription blocked Xbra expression during gastrula stages (Fig. 7G). By contrast, when treatment started in the late blastula, after the onset of Xbra expression, further expression was barely reduced (Fig. 7H). However, when combined with a sub-threshold dose of EphA4-MO, late blastula SU5402 treatment was effective (Fig. 7I), consistent with a cross-activation of EphA4 and FGF receptors (Yokota et al., 2003; Park et al., 2004). Thus, EphA4 is normally necessary and sufficient for Xbra induction, but, at low EphA4 levels, its support by FGF signaling becomes apparent.

Both MAP kinase (Umbhauer et al., 1995; Northrop et al., 1995) and PI3K signaling (Carballada et al., 2001) have been implicated in FGF-dependent Xbra expression. We tested whether any of these pathways is also involved in EphA4/Pak1-dependent Xbra regulation. Surprisingly, the MAP kinase inhibitor U0126 never interfered with Xbra expression (supplementary material Fig. S3B,C), although it affected gastrulation (our unpublished results). This suggests that MAPK, a possible effector of Pak1 (Bokoch, 2003), is not involved in EphA4/Pak1 signaling in the dorsal lip. The PI3K

Development (2014) 141, 3649-3661 doi:10.1242/dev.111880

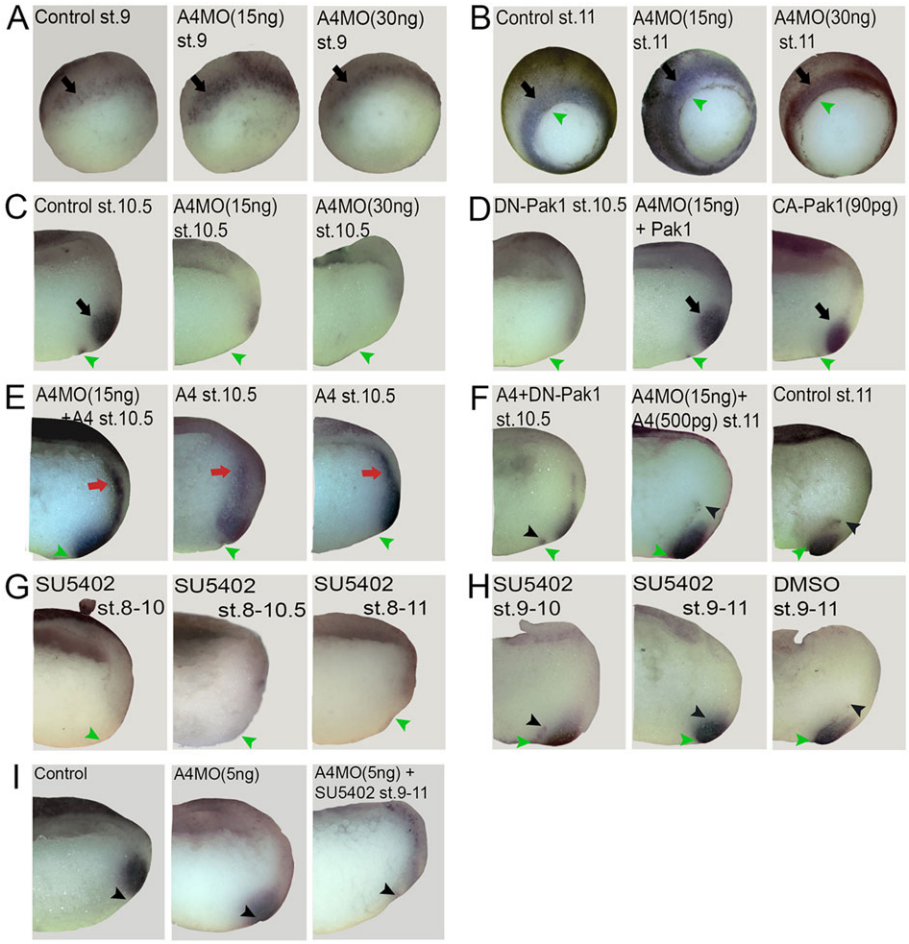

Fig. 7. *Xbra* expression as detected by *in situ* hybridization. Treatments and stages indicated in A-I. Black arrowheads, positions of bottle cells; green arrowheads, blastopore; black arrows, *Xbra* expression in lip region; red arrows, ectopic *Xbra* expression in anterior mesoderm or BCR.

inhibitor LY294002 prevented expression early, but not during EphA4/Pak1 signaling after the initial gastrula stage (supplementary material Fig. S3D). None of these pathways seems to mediate EphA4-dependent Xbra expression.

Xbra expression is required for peak involution

Inhibition of Xbra function with dominant-negative enRXbra abrogates involution, but as the construct also abolishes mesoderm induction, this effect is likely to be a consequence of cell fate changes (Conlon and Smith, 1999). Our finding that a transient downregulation of Xbra expression is correlated with defective involution in the absence of noticeable fate changes suggests a direct role for Xbra in peak involution. However, co-injection of *Xbra* mRNA with EphA4-MO did not rescue involution (supplementary material Fig. S4A,B). As *Xbra* mRNA alone also impeded involution (supplementary material Fig. S4A,B), the inability to rescue could be due to a mis-expression of Xbra from early stages on and in all descendants of the injected blastomeres (Kwan and Kirschner, 2003).

To reduce such side effects, we first restricted the time of Xbra function by activating hormone-inducible Xbra-GR with dexamethasone (DEX) at different stages. DEX treatment of uninjected embryos, or expression of Xbra-GR without DEX application, had no effect, although both treatments combined reduced archenteron formation (Fig. 8A,B). In EphA4 morphants, *Xbra-GR* mRNA injection followed by DEX treatment at stage 9 did not rescue an archenteron, but treatment at stage 10 was effective (Fig. 8A,B). Folding of lip-BCR explants was also rescued by DEX/Xbra-GR (Fig. 8C,D). In a second approach, we showed that Xbra can rescue involution in Pak1-inhibited explants when most tissue normally not expressing Xbra is removed. In lip-BCR explants, rescue was weak (Fig. 8E,F). In lip-only explants, involution was strongly inhibited by DN-Pak1, but only weakly by Xbra. Co-expression of Xbra with DN-Pak1 promoted a robust rescue (Fig. 8G,H). Thus, the fine-tuned expression of Xbra is required for peak involution.

Its requirement for peak involution and for the bending of the Xbra domain suggests a tissue-autonomous function of Xbra. Indeed, the Gsc domain is not affected by interference with EphA4/Pak1/Xbra. *In situ* hybridization indicates an inward movement of Gsc-expressing cells despite EphA4 or Pak1 inhibition (see Fig. 4A; supplementary material Fig. S2). Also, radial intercalation in open-faced mesoderm explants that corresponds to the internalization of Gsc cells does not depend on Pak1 (Fig. 8I; supplementary material Movie 7). By contrast, the asymmetric elongation of Xbra domain explants by radial convergence (Fig. 8J,J′) is blocked by EphA4 knockdown and rescued by Pak1 (Fig. 8K,L,N). Thus, the behavior of the Xbra domain itself is regulated by EphA4/Pak1-dependent Xbra expression. Ectodermal control explants do not elongate asymmetrically (Fig. 8M-N).

EphrinB2 is required for peak involution

Ectopic Xbra expression in EphA4-injected BCR at sites of contact with mesoderm suggested that an EphA4 ligand is present in the mesoderm. Consistent with this, mesoderm induced Xbra in EphA4-injected dorsal, though not ventral, BCR explants; vegetal

Development (2014) 141, 3649-3661 doi:10.1242/dev.111880

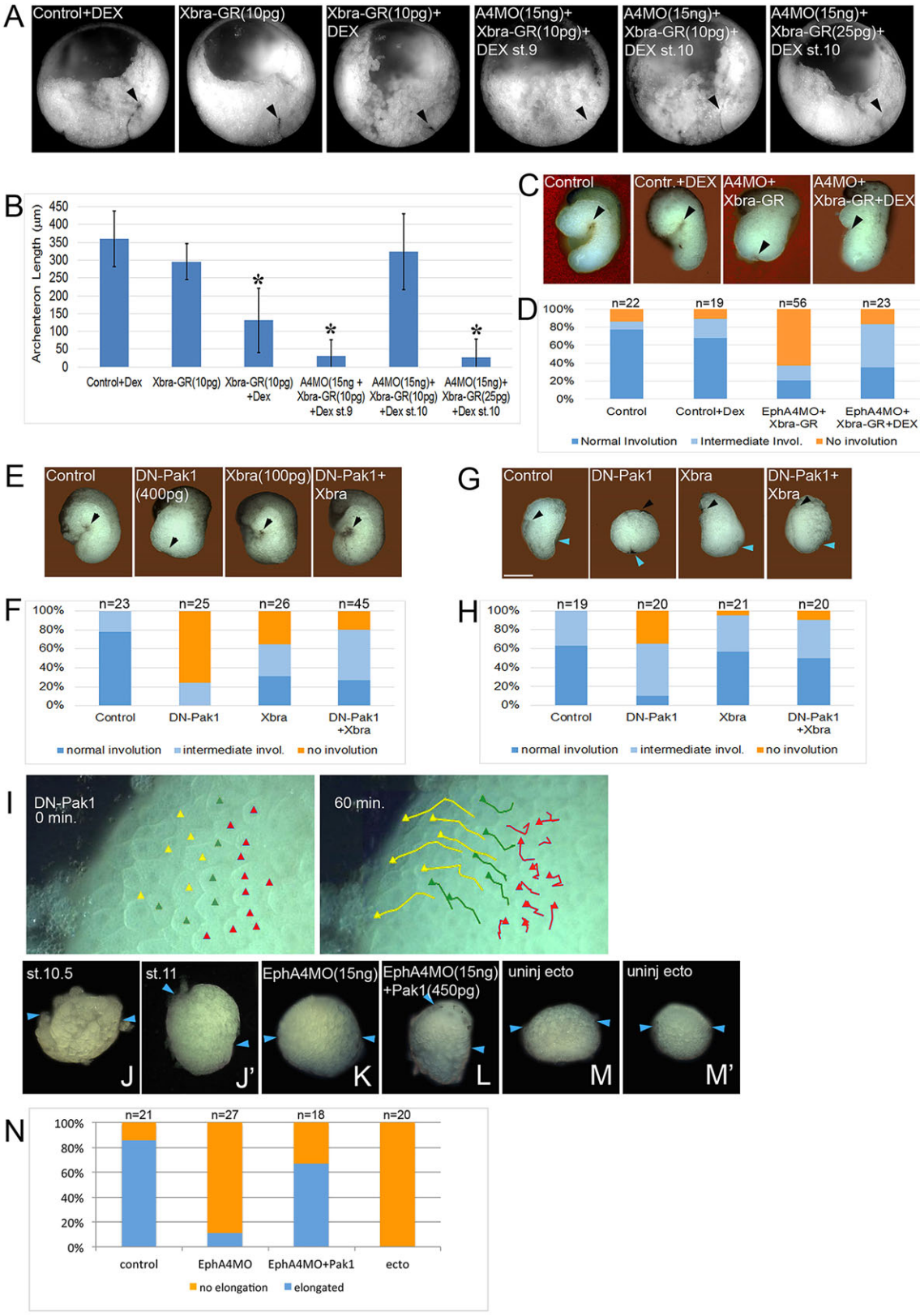

Fig. 8. Xbra acts downstream of EphA4/Pak1. (A) Embryos fractured sagittally after peak involution (stage 11); rescue of archenteron formation by Xbra-GR/dexamethasone (DEX). Arrowheads, end of archenteron. (B) Archenteron lengths; n, number of embryos; bars indicate s.d.; asterisks indicate significance levels at least $P<0.05$. (C,D) Lip-BCR explants, rescue of folding by Xbra-GR; n, number of explants. (E,F) Lip-BCR explants, rescue of folding by *Xbra* mRNA injection after Pak1 inhibition; n, number of explants. (G,H) Rescue of lip-only morphology by *Xbra* mRNA injection after Pak1 inhibition; n, number of explants. (I) Migration of cells in anterior open-faced explants (yellow and green arrows) is not inhibited by DN-Pak1. Red arrows, random motility in Xbra domain. (J-N) Asymmetric elongation in Xbra domain explants (J,J′) is inhibited by EphA4 knockdown (K) and rescued by Pak1 (L); no elongation in ectoderm explants of different sizes (M,M′). Scale bars: 100 µm.

Development (2014) 141, 3649-3661 doi:10.1242/dev.111880

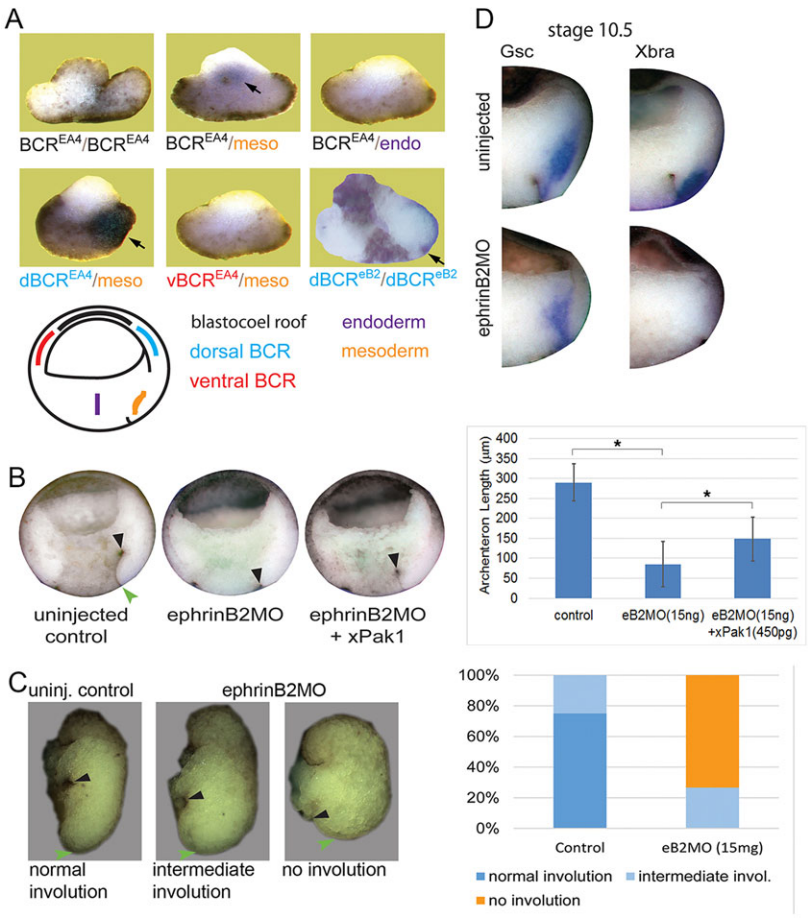

Fig. 9. Ephrin-B2 is required for peak involution. (A) Mesoderm induces *Xbra* in EphA4-expressing dorsal BCR. Tissues were combined at initial gastrula stage and fixed 2 h later (stage 10.5) for *in situ* hybridization. Arrows, *Xbra* expression. (B) Embryos fractured sagittally after peak involution (stage 11); inhibition of archenteron elongation by ephrinB2-MO; bars indicate s.d.; asterisks indicate significance levels at least $P<0.05$. (C) Inhibition of Lip-BCR explants folding by ephrin B2-MO. Green arrowheads, tip of blastopore lip; black arrowheads, position of bottle cells. (D) *In situ* hybridization for Gsc, Xbra in ephrinB2-MO embryos.

cell mass was ineffective in this assay (Fig. 9A). EphA4 also induced Xbra when overexpressed in anterior mesoderm (see Fig. 7E). These findings suggest that an EphA4 ligand in the mesoderm elicits Xbra expression where it overlaps with EphA4.

EphrinB2 is a known EphA4 ligand (Blits-Huizinga et al., 2004), and its transcripts are enriched in mesoderm (Rohani et al., 2011). Its knockdown with ephrinB2-MO (Rohani et al., 2011) diminished archenteron formation, but *Pak1* mRNA rescued it to some extent (Fig. 9B), consistent with a role of ephrinB2 in the EphA4 pathway. Likewise, in lip-BCR explants from ephrinB2 morphants, involution was inhibited (Fig. 9C) and Xbra expression in the dorsal marginal zone was downregulated in the early gastrula (Fig. 9D), indicating that ephrinB2 is necessary for both Xbra expression and peak involution. Ectopic expression of ephrinB2 in the dorsal BCR alone is sufficient for Xbra expression (Fig. 9A), possibly owing to interactions with other Eph receptors in the BCR.

Transient Xbra downregulation is compatible with subsequent convergent extension

Although the transient downregulation of Xbra expression interferes with involution, convergent extension resumes in the middle to late gastrula as Xbra expression returns to normal in EphA4 morphants. Blastopore lips from EphA4-MO embryos elongate, although convergence is reduced (Park et al., 2011). Late gastrula convergent extension in involution-compromised embryos was further examined in Pak1-inhibited embryos.

DN-Pak1 initially blocks archenteron formation, but later a shortened archenteron and dorsal axis develop (Nagel et al., 2009) (Fig. 10A,B). The lack of previous involution affects the axis. Chordin is normally expressed in anterior chordamesoderm, but not posteriorly in the lip. By contrast, in DN-Pak1 embryos expression extends into the lip, suggesting that anterior chordamesoderm forms now the posterior end of the tissue (Fig. 10A). Moreover, chordamesoderm normally extends in parallel with the BCR from which it is separated by Brachet's cleft. The cleft is present in normal lip-BCR explants, but DN-Pak1 explants elongate as a solid mass (Fig. 10C). Thus, convergent extension occurs after a transient downregulation of Xbra and in the absence of peak involution, but its topology is altered and larvae develop posterior truncations (Fig. 10D). Two phases of convergent extension can thus be distinguished: one associated with involution, the other occurring in post-involution dorsal mesoderm in parallel to neural convergence and extension. The first phase is subdivided into an early stage driven by differential migration in the Gsc domain, and a later stage that adds the bending of the Xbra domain by radial convergence.

DISCUSSION

We showed that peak involution of the dorsal mesoderm comprises two components: a wave of active bending of the mesoderm that spreads from anterior to posterior; and a simultaneous anteroposterior (vegetal-animal) elongation and mediolateral narrowing of the lip region, which together constitute an early phase of convergent extension. Both the differential migration of cells in the Gsc domain and the active bending of the Xbra domain by radial convergence contribute to peak involution. Xbra is necessary in this process; its expression depends on EphA4, the Eph ligand ephrinB2 and the effector Pak.

Development (2014) 141, 3649-3661 doi:10.1242/dev.111880

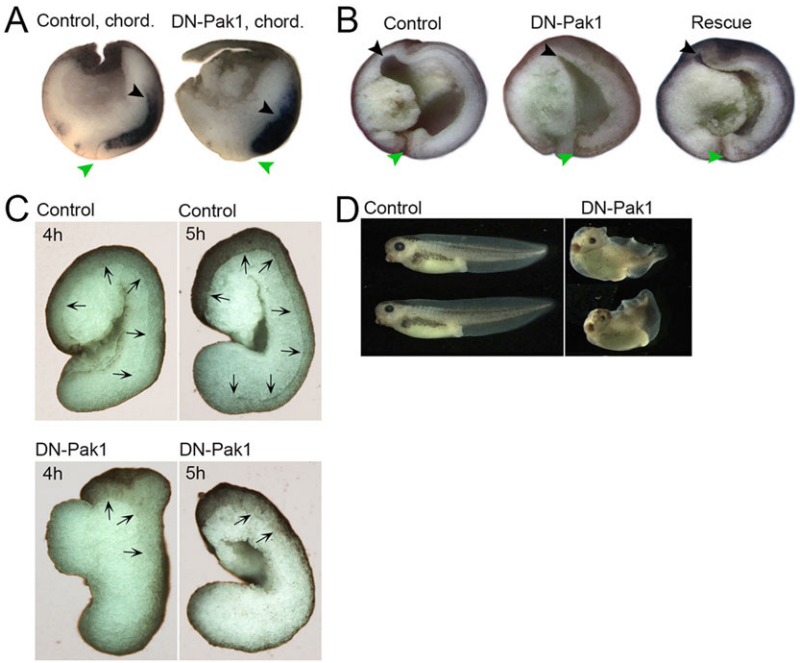

Fig. 10. Resumption of convergent extension after failed involution. (A) Chordin expression in control and DN-Pak1-injected embryos in late gastrula (stage 12). (B) Archenteron after completion of gastrulation in control and Pak1-inhibited embryos. Black arrowheads, positions of bottle cells; green arrowheads, blastopore. (C) Control and Pak1-inhibited lip-BCR explants cultured for 4 and 5 h, respectively. Arrows, Brachet's cleft separating BCR and mesoderm. (D) Control and Pak1-inhibited larvae.

Geometry of involution

Some of the complexity of involution can be understood from geometrical constraints of the process. First, any bending in a continuous cell sheet requires two complementary changes in sheet curvature: as a region bends inwards, the zone peripheral to it must curve in the opposite direction. During invagination, the first of these bending events is typically an active process, and it is usually implied that counter-bending at the periphery occurs as a passive consequence. However, sheet folding during involution is in fact an integrated process, the components of which – bending at the vegetal-marginal zone boundary and counter-bending within the Xbra domain – both occur autonomously in isolated tissue fragments. Similarly, in the newt *Cynops pyrrhogaster*, explants of the dorsal epithelial layer fold into an S-shape at two analogous inflection points, recapitulating internalization *in vitro* (Komazaki, 1993).

Second, the thickness of the involuting tissue, together with the spherical shape of the gastrula, necessitates specific deformations of the lip. When laterally separated lip cells move from the surface to the interior, their radial trajectories converge towards the animal-vegetal axis of the embryo, and the eventual distance between the cells will be 0.6 times that of the initial distance (Fig. 11A). This mediolateral convergence of the lip as it rotates inward is translated into an extension in the direction of movement (Fig. 11B). As convergence is strongest at the surface, extension must be strongest there too, and more superficial cells must move faster and bypass deeper cells. By approximating the lip by a quadrant of a disc rotating inward by 90° (Fig. 11B), we estimated that it should elongate by 50 µm, which agrees well with the rate of explant elongation during peak involution (Wilson and Keller, 1991; Ninomiya and Winklbauer, 2008). These considerations accurately predict the active shape changes of lip explants, which had previously been described as the first phase of convergent extension.

Altogether, the complex geometrical requirements of involution are met by a striking autonomy of tissue movements. Peak involution is driven neither solely by a mediolateral hoop stress, with involution as a passive consequence, nor by radial cell movement, with convergence being forced upon the tissue by spatial constraints. Instead, both the radial and mediolateral components of involution seem to be programmed. Likewise, bending and counter-bending are both autonomous processes. In general, geometrically required shape changes are not passive consequences of a dominant,

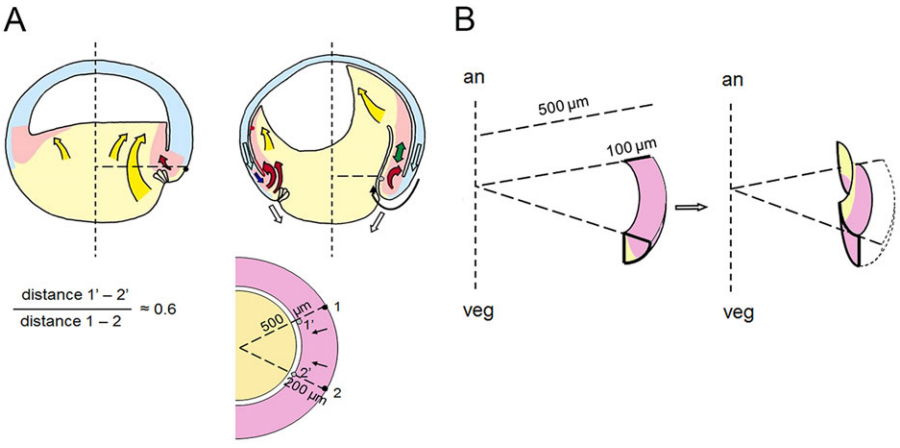

Fig. 11. Geometry of dorsal involution. (A) Involution in context of gastrulation. Top: movements at early and mid-gastrula stages. Yellow, endoderm; red, mesoderm; blue, ectoderm; yellow arrows, vegetal rotation; red arrows, involution; blue arrows, epiboly; green double-arrow, late-stage convergent extension; white arrows, vegetal displacement of lips during blastopore constriction; vertical dashed line, animal-vegetal axis. Bottom: horizontal section at level of horizontal dashed lines in top, dorsal side. Dashed lines connect surface cells 1 and 2 to animal-vegetal axis, over a distance of 500 µm, thickness of mesoderm layer 200 µm. As cells internalize, they converge by a factor of 0.6. (B) Deduced deformation of a segment of the lip during peak involution; colors as in Fig. 3E.

Development (2014) 141, 3649-3661 doi:10.1242/dev.111880

leading process here, but are programmed as independent movements that fit together in a mosaic-like fashion.

Cellular basis of involution

Two regions of the dorsal blastopore lip can be discerned on the basis of marker gene expression, cell shape, cell behavior and the response to EphA4/Pak1/Xbra inhibition, and both the Gsc-expressing prechordal mesoderm and Xbra-expressing chordamesoderm contribute through specific cellular mechanisms to peak involution.

In the Gsc domain, cells are initially aligned along vegetal-to-animally directed arcs, suggesting migration on trajectories similar to those of ventral blastopore lip cells (Ibrahim and Winklbauer, 2001). After internalization, cells reorient themselves perpendicular to the BCR to engage in PDGF-directed intercalation and movement towards the BCR. When PDGF signaling is inhibited, cells fall back into their vegetal-animal orientation parallel to the adjacent endoderm cells. This suggests a default orientation throughout gastrulation by an unknown mechanism, common to both prechordal mesoderm and endoderm cells (Damm and Winklbauer, 2011).

Part of the Gsc domain is already deep within the embryo at the onset of gastrulation, but its outer part has still to move through the blastopore lip, requiring convergence and extension. How is the animally/anteriorly oriented migration in this domain reconciled with the necessary mediolateral and radial cell intercalation? We propose that differential migration of cells, i.e. their movement in the same direction but at different velocities, generates intercalation perpendicular to the direction of migration. This can be observed in open-faced lip explants, in which convergent extension is initiated by cell intercalation in the Gsc domain. Intercalation in this region is directional (Wilson and Keller, 1991), with deeper cells appearing at gaps between cells that move apart anteroposteriorly due to differences in velocity. Likewise, cells move laterally into gaps between anteroposteriorly separating cells, like cars merging into fewer lanes on a highway. This mechanism should suffice to generate convergent extension of the Gsc domain.

Cells in the Gsc domain migrate inwards from the onset of gastrulation to the end of peak involution, as indicated by their movement in explants (Wilson and Keller, 1991; Keller et al., 1992; this paper) and by cell morphology. This internalization of the Gsc domain is independent of the rest of involution: in EphA4- or Pak1-inhibited embryos, the Gsc domain extends animally along the BCR, although neither the epithelial layer nor the Xbra domain follows. Instead, the domain stretches to remain in contact with the epithelial layer. Thus, the inward movement of the Gsc domain does not depend on EphA4/Pak1 function, but it is not sufficient to drive peak involution.

In the Xbra domain, cells adjacent to the epithelial layer begin to engage in mediolateral intercalation behavior at the onset of peak involution (Shih and Keller, 1992; Lane and Keller, 1997), which is likely to contribute to involution-associated mediolateral convergence. The most striking process, however, is the autonomous bending of the Xbra domain by radial convergence, such that the point of highest lip curvature shifts from the Gsc-Xbra boundary to within the Xbra domain. This shape change is asymmetrical and elongates the Xbra domain at its internalized side. The cellular basis of this movement remains to be identified. Possibly, mediolateral differential cell intercalation generates here the same overall effects as anteroposterior differential migration does in the Gsc domain. To what degree interaction with the epithelial layer contributes to Xbra domain bending likewise remains to be determined.

Brachyury function at the blastopore

The *Brachyury* gene is common to metazoans, and its early expression occurs typically at the blastopore or related structures (Technau, 2001; Marcellini, 2006; Sebe-Pedros et al., 2013), suggesting a role in gastrulation. For example, in sea urchins, Brachyury is expressed at the outer rim of the blastopore (Hibino et al., 2004), and its inhibition leads to defects consistent with a role in involution (Gross and McClay, 2001). Brachyury is also associated with involution in the primitive chordate *Branchiostoma* (Zhang et al., 1997). Beyond its morphogenetic role, Brachyury has been implicated in the specification of parts of the endoderm and mesoderm (reviewed by Showell et al., 2004).

In *Xenopus*, Xbra sequentially controls mesoderm specification, involution including early convergent extension, and post-involution convergent extension; its expression is separately controlled during these phases. For pre-gastrular posterior mesoderm specification, Xbra expression depends on FGF, nodal and Wnt signaling (Smith et al., 1991; Cunliffe and Smith, 1992; Hemmati-Brivanlou and Melton, 1992; Amaya et al., 1993; Vonica and Gumbiner, 2002; Schohl and Fagotto, 2003). We confirmed that this early expression depends on PI3K signaling (Carballada et al., 2001), whereas, surprisingly, inhibition of MAP kinase had no effect. In the late gastrula, Xbra is required for convergent extension of axial mesoderm. Expression is again controlled by FGF signaling (Isaacs et al., 1994; Schulte-Merker and Smith, 1995; Silva Casey et al., 1998; Yokota et al., 2003). We inserted an additional phase of Xbra function, the control of peak involution on the dorsal side of the mid-gastrula, when Xbra is controlled by EphA4/ephrinB2/Pak. Whether Xbra also plays a role in the involution or convergent thickening of the ventral lip (Keller and Danilchik, 1988) remains to be seen.

Although occurring in three phases, Xbra expression appears continuous in *Xenopus*, but in the slow-developing frog, *Colostethus machalilla* (now *Epipedobates machalilla*), phases are separated (Benitez and del Pino, 2002). The ring-shaped expression of Brachyury in the blastula marginal zone disappears, to be replaced later by expression in the constricting blastopore; still later, after blastopore closure, Brachyury expression appears in the prospective notochord, suggesting that a tri-phasic Brachyury expression pattern could be ancestral for anurans. In the urodeles *Cynops* and *Ambystoma*, Brachyury is expressed late, after the Gsc-expressing anterior mesoderm has involuted, but in time for the involution of the Brachyury-expressing posterior mesoderm (Kaneda et al., 2009; Swiers et al., 2010). It remains to be determined, however, whether a role in germ layer internalization is indeed a common feature of the amphibian or even the metazoan *Brachyury* gene.

MATERIALS AND METHODS

Embryos, injections, treatments

Xenopus laevis embryos were obtained and injected as described (Luu et al., 2008). EphA4 MO, 5′-CGGAGGTGGATTAAGAGATGCCTAT-3′ (Park et al., 2011) and ephrinB2-MO, 5′-ACACCGAGTCCCCGCTCAGTGCC-AT-3′ (Rohani et al., 2011) were obtained from Genetools. Mouse and *Xenopus* EphA4 in pCS2^{+} (T. Moss, Université Laval, Quebec, Canada) were cut with *Xba*I, and mouse kinase dead EphA4 (I. Daar, National Cancer Institute, Frederick, MD, USA) with *Not*1, and were transcribed using SP6 polymerase. *Xenopus* Pak1, a kinase-dead mutant (KD-Pak1) in pT7TS and constitutively active CA-Pak1 in pTSHAxPAK1 (T. Moss) were linearized with *Xba*I and transcribed with T7 polymerase (Bisson et al., 2003, 2007). *Xenopus* Brachyury (Xbra) and Xbra-GR in pSP64T (Conlon et al., 1996; provided by J. Smith, University of Cambridge, UK) were linearized with *Hin*dIII or *Sal*1, respectively, and transcribed with SP6 polymerase. Constitutively active CA-Mek in pSP64 (M. Whitman, Harvard Medical

Development (2014) 141, 3649-3661 doi:10.1242/dev.111880

School, Boston, MA, USA) was lineralized with *Eco*R1 and transcribed with SP6. Inhibitors SU5402, U0126 (EMD) and LY294002 (Sigma-Aldrich), were dissolved in DMSO. Embryo surface was labeled by biotinylation and Cy3-labeled anti-biotin antibody staining according to the manufacturer's instructions (Sigma-Aldrich).

Microsurgery

Microsurgery was performed in modified Barth's saline (MBS; Winklbauer, 1988). Explants were of the thickness of the BCR and extended 40-45° on either side of the dorsal midline. They were filmed in MBS at 1 frame/min from above or in side view in a 45° mirror, or fixed in 4% formaldehyde in MBS and fractured mid-sagittally for photography or *in situ* hybridization.

In situ hybridization

In situ hybridization was modified after Harland (1991). Gsc pBluescript SK(−) (Cho et al., 1991; gift from H. Steinbeisser, University of Heidelberg, Germany) was linearized with *Eco*R1, Xbra DB30 pSP73 (M. Sargent, National Institute for Medical Research, London, UK) with *Bgl*2, Sox2 pCS2-Sox2 with *Eco*RI (Mizuseki et al. 1998; gift from Y. Sasai, Riken Institute, Kobe, Japan), Cer pBSSK, Chd clone H7 in pBluescript SK(−) (E. DeRobertis, University of California, Los Angeles, CA, USA) with *Eco*R1. Digoxigenin-labeled antisense probe, synthesized using T7 RNA polymerase (mMessage mMachine, Ambion), was detected with BM Purple (Roche).

Image processing

Photographs of embryos and explants in Fig. 1A-F, Fig. 2G,H, Fig. 4A-C, Fig. 5A,C,D, Fig. 6A,B,D,F,H, Fig. 7A-I, Fig. 8A,C,E,G,J-M, Fig. 9A-D and Fig. 10A-C have been post-processed to place the images on consistent backgrounds and to ensure consistent display in terms of orientation.

Scanning electron microscopy

Embryos were fixed in 2.5% glutaraldehyde/0.1 M sodium cacodylate overnight at 4°C, post-fixed in osmium tetraoxide and dehydrated in ethanol/0.1 M cacodylate and ethanol/hexamethyldisilizane series. Specimens were dried overnight and sputter-coated with gold-palladium. The experiments involving *X. laevis* embryos conform to the regulatory standards of the University of Toronto, Canada.

Acknowledgements

We thank H. Ninomiya for surface-biotinylated embryos, T. Moss, J. Smith, M. Whitman, H. Steinbeisser, M. Sargent, Y. Sasai, E. DeRobertis and I. Daar for reagents, and D. Shook for critical comments on the manuscript.

Competing interests

The authors declare no competing financial interests.

Author contributions

R.W. conceived the study, designed experiments and wrote the manuscript. S.E., J.W.H.W., O.L., E.W.D. and R.W. performed the experiments. M.N. analyzed the data.

Funding

Funding was provided by the Natural Sciences and Engineering Research Council of Canada and the Canadian Institutes of Health Research [grant MOP-53075].

Supplementary material

Supplementary material available online at http://dev.biologists.org/lookup/suppl/doi:10.1242/dev.111880/-/DC1

References

Amaya, E., Stein, P. A., Musci, T. J. and Kirschner, M. W. (1993). FGF signaling in the early specification of mesoderm in Xenopus. *Development* **118**, 477-487.

Benítez, M.-S. and del Pino, E. M. (2002). Expression of Brachyury during development of the dendrobatid frog Colostethus machalilla. *Dev. Dyn.* **225**, 592-596.

Bisson, N., Islam, N., Poitras, L., Jean, S., Bresnick, A. and Moss, T. (2003). The catalytic domain of xPAK1 is sufficient to induce myosin II dependent in vivo cell fragmentation independently of other apoptotic events. *Dev. Biol.* **263**, 264-281.

Bisson, N., Poitras, L., Mikryukov, A., Temblay, M. and Moss, T. (2007). EphA4 signaling regulates blastomere adhesion in the Xenopus embryo by recruiting Pak1 to suppress Cdc42 function. *Mol. Biol. Cell* **18**, 1030-1043.

Blits-Huizinga, C. T., Nelersa, C. M., Malhotra, A. and Liebl, D. J. (2004). Ephrins and their receptors: binding versus biology. *IUBMB Life* **56**, 257-265.

Bokoch, G. M. (2003). Biology of the p21-activated kinases. *Ann. Rev. Biochem.* **72**, 743-781.

Carballada, R., Yasuo, H. and Lemaire, P. (2001). Phosphatidylinositol-3 kinase acts in parallel to the ERK MAP kinase in the FGF pathway during Xenopus mesoderm induction. *Development* **128**, 35-44.

Cau, J., Faure, S., Vigneron, S., Labbe, J. C., Delsert, C. and Morin, N. (2000). Regulation of Xenopus p21-activated kinase (X-PAK2) by Cdc42 and maturation-promoting factor controls Xenopus oocyte maturation. *J. Biol. Chem.* **275**, 2367-2375.

Cho, K. W. Y., Blumberg, B., Steinbeisser, H. and De Robertis, E. M. (1991). Molecular nature of Spemann's organizer: the role of the Xenopus homeobox gene goosecoid. *Cell* **67**, 1111-1120.

Conlon, F. L. and Smith, J. C. (1999). Interference with Brachyury function inhibits convergent extension, causes apoptosis, and reveals separate requirements in the FGF and activin signalling pathways. *Dev. Biol.* **213**, 85-100.

Conlon, F. L., Sedgwick, S. G., Weston, K. M. and Smith, J. C. (1996). Inhibition of Xbra transcription activation causes defects in mesodermal patterning and reveals autoregulation of Xbra in dorsal mesoderm. *Development* **122**, 2427-2435.

Cunliffe, V. and Smith, J. C. (1992). Ectopic mesoderm formation in Xenopus embryos caused by widespread expression of a Brachyury homolog. *Nature* **358**, 427-430.

Damm, E. W. and Winklbauer, R. (2011). PDGF-A controls mesoderm cell orientation and radial intercalation during *Xenopus* gastrulation. *Development* **138**, 565-575.

Ewald, A. J., Peyrot, S. M., Tyszka, J. M., Fraser, S. E. and Wallingford, J. B. (2004). Regional requirements for Dishevelled signaling during Xenopus gastrulation: separable effects on blastopore closure, mesendoderm internalization and archenteron formation. *Development* **131**, 6195-6209.

Fletcher, R. B. and Harland, R. M. (2008). The role of FGF signaling in the establishment and maintenance of mesodermal gene expression in Xenopus. *Dev. Dyn.* **237**, 1243-1254.

Gross, J. M. and McClay, D. R. (2001). The role of Brachyury (T) during gastrulation movements in the sea urchin Lytechinus variegatus. *Dev. Biol.* **239**, 132-147.

Hardin, J. and Keller, R. (1988). The behavior and function of bottle cells during gastrulation of Xenopus laevis. *Development* **103**, 211-230.

Harland, R. (1991). In situ hybridization: an improved whole-mount method for Xenopus embryos. *Methods Cell Biol.* **36**, 685-695.

Hemmati-Brivanlou, A. and Melton, D. A. (1992). A truncated activin receptor inhibits mesoderm induction and formation of axial structures in Xenopus embryos. *Nature* **359**, 609-614.

Hibino, T., Harada, Y., Minokawa, T., Nonaka, M. and Amemiya, S. (2004). Molecular heterotopy in the expression of Brachyury orthologs in order Clypeasteroidea (irregular sea urchins) and oder Echinoidea (regular sea urchins). *Dev. Genes Evol.* **214**, 546-558.

Hofmann, C., Shepelev, M. and Chernoff, J. (2004). The genetics of Pak. *J. Cell Sci.* **117**, 4343-4354.

Hwang, Y.-S., Lee, H.-S., Kamata, T., Mood, K., Cho, H. J., Winterbottom, E., Ji, Y. J., Singh, A. and Daar, I. O. (2013). The Smurf ubiquitin ligases regulate tissue separation via antagonistic interactions with ephrinB1. *Genes Dev.* **27**, 491-503.

Ibrahim, H. and Winklbauer, R. (2001). Mechanisms of mesendoderm internalization in the Xenopus gastrula: lessons from the ventral side. *Dev. Biol.* **240**, 108-122.

Isaacs, H. V., Pownall, M. E. and Slack, J. M. W. (1994). eFGF regulates Xbra expression during Xenopus gastrulation. *EMBO J.* **13**, 4469-4481.

Islam, N., Poitras, L. and Moss, T. (2000). The cytoskeletal effector xPAK1 is expressed during both ear and lateral line development in Xenopus. *Int. J. Dev. Biol.* **44**, 245-248.

Kaneda, T., Iwamoto, Y. and Motoki, J.-Y. D. (2009). Origin of the prechordal plate and patterning of the anteroposterior regional specificity of the involuting and extending archenteron roof of a urodele, Cynops pyrrhogaster. *Dev. Biol.* **334**, 84-96.

Keller, R. E. (1980). The cellular basis of epiboly: an SEM study of deep-cell rearrangement during gastrulation in Xenopus laevis. *J. Embryol. Exp. Morph.* **60**, 201-234.

Keller, R. E. (1981). An experimental analysis of the role of bottle cells and the deep marginal zone in gastrulation of Xenopus laevis. *J. Exp. Zool.* **216**, 81-101.

Keller, R. and Danilchik, M. (1988). Regional expression, pattern and timing of convergence and extension during gastrulation of Xenopus laevis. *Development* **103**, 193-209.

Keller, R., Shih, J. and Domingo, C. (1992). The patterning and functioning of protrusive activity during convergence and extension of the Xenopus organizer. *Development 1992 Suppl.*, 81-91.

Komazaki, S. (1993). Movement of an epithelial layer isolated from early embryos of the newt, Cynops pyrrhogaster. II. Formation of a blastoporal groove and archenteron in a superficial epithelial layer isolated from initial gastrula. *Dev. Growth Differ.* **35**, 471-478.

Kwan, K. M. and Kirschner, M. W. (2003). Xbra functions as a switch between cell migration and convergent extension in the Xenopus gastrula. *Development* **130**, 1961-1972.
Lane, M. C. and Keller, R. (1997). Microtubule disruption reveals that Spemann's organizer is subdivided into two domains by the vegetal alignment zone. *Development* **124**, 895-906.
Lu, W., Katz, S., Gupta, R. and Mayer, B. J. (1997). Activation of Pak by membrane localization mediated by an SH3 domain from the adaptor protein Nck. *Curr. Biol.* **7**, 85-94.
Luu, O., Nagel, M., Wacker, S., Lemaire, P. and Winklbauer, R. (2008). Control of gastrula cell motility by the Goosecoid/Mix.1/Siamois network: basic patterns and paradoxical effects. *Dev. Dyn.* **237**, 1307-1320.
Marcellini, S. (2006). When Brachyury meets Smad1: the evolution of bilateral symmetry during gastrulation. *BioEssays* **28**, 413-420.
Mizuseki, K., Kishi, M., Matsui, M., Nakanishi,, S. and Sasai, Y. (1998). Xenopus Zic-related-1 and Sox-2, two factors induced by chordin, have distinct activities in the initiation of neural induction. *Development* **125**, 579-587.
Nagel, M., Luu, O., Bisson, N., Macanovic, B., Moss, T. and Winklbauer, R. (2009). Role of p21-activated kinase in cell polarity and directional mesendoderm migration in the Xenopus gastrula. *Dev. Dyn.* **238**, 1709-1726.
Ninomiya, H. and Winklbauer, R. (2008). Epithelial coating controls mesenchymal shape change through tissue-positioning effects and reduction of surface-minimizing tension. *Nat. Cell Biol.* **10**, 61-69.
Northrop, J., Woods, A., Seger, R., Suzuki, A., Ueno, N., Krebs, E. and Kimelman, D. (1995). BMP-4 regulates the dorsal-ventral differences in FGF/MAPKK-mediated mesoderm induction in Xenopus. *Dev. Biol.* **172**, 242-252.
Park, E. K., Warner, N., Bong, Y.-S., Stapleton, D., Maeda, R., Pawson, T. and Daar, I. O. (2004). Ectopic EphA4 receptor induces posterior protrusions via FGF signaling in Xenopus embryos. *Mol. Biol. Cell* **15**, 1647-1655.
Park, E. C., Cho, G.-S., Kim, G.-H., Choi, S.-C. and Han, J.-K. (2011). The involvement of Eph-ephrin signaling in tissue separation and convergence during Xenopus gastrulation movements. *Dev. Biol.* **350**, 441-450.
Rhumbler, L. (1902). Zur Mechanik der Gastrulationsvorgange, insbesondere der Invagination. Eine entwicklungsmechanische Studie. *W. Roux' Arch. Entw. Mech. Org.* **14**, 401-476.
Rohani, N., Canty, L., Luu, O., Fagotto, F. and Winklbauer, R. (2011). EphrinB/EphB-signaling controls embryonic germ layer separation by contact-induced cell detachment. *PLoS Biol.* **9**, e1000597.
Schohl, A. and Fagotto, F. (2003). A role for maternal β-catenin in early mesoderm induction in Xenopus. *EMBO J.* **22**, 3303-3313.
Schulte-Merker, S. and Smith, J. C. (1995). Mesoderm formation in response to Brachyury requires FGF signalling. *Curr. Biol.* **5**, 62-67.
Sebe-Pedros, A., Ariza-Cosano, A., Weirauch, M. T., Leininger, S., Yang, A., Torruella, G., Adamski, M., Adamska, M., Hughes, T. R., Gomez-Skarmeta, J. L. et al. (2013). Early evolution of the T-box transcription factor family. *Proc. Natl. Acad. Sci. USA* **110**, 16050-16055.
Shih, J. and Keller, R. (1992). Patterns of cell motility in the organizer and dorsal mesoderm of Xenopus laevis. *Development* **116**, 915-930.
Showell, C., Binder, O. and Conlon, F. L. (2004). T-box genes in early embryogenesis. *Dev. Dyn.* **229**, 201-218.
Silva Casey, E., O'Reilly, M.-A. J., Conlon, F. L. and Smith, J. C. (1998). The T-box transcription factor Brachyury regulates expression of eFGF through binding to a non-palindromic response element. *Development* **125**, 3887-3894.
Smith, J. C., Price, B. M. J., Green, J. B. A., Weigel, D. and Herrmann, B. G. (1991). Expression of a Xenopus homolog of Brachyury (T) is an immediate-early response to mesoderm induction. *Cell* **67**, 79-87.
Souopgui, J., Sölter, M. and Pieler, T. (2002). Xpak3 promotes cell cycle withdrawal during primary neurogenesis in Xenopus laevis. *EMBO J.* **21**, 6429-6439.
Swiers, G., Chen, Y.-H., Johnson, A. D. and Loose, M. (2010). A conserved mechanism for vertebrate mesoderm specification in urodele amphibians and mammals. *Dev. Biol.* **343**, 138-152.
Tanaka, M., Wang, D.-Y., Kamo, T., Igarashi, H., Wang, Y., Xiang, Y.-Y., Tanioka, F., Naito, Y. and Sugimura, H. (1998). Interaction of EphB2-tyrosine kinase receptor and its ligand conveys dorsalization signal in Xenopus laevis development. *Oncogene* **17**, 1509-1516.
Technau, U. (2001). Brachyury, the blastopore and the evolution of the mesoderm. *BioEssays* **23**, 788-794.
Umbhauer, M., Marshall, C. J., Mason, C. S., Old, R. W. and Smith, J. C. (1995). Mesoderm induction in Xenopus caused by activation of MAP kinase. *Nature* **376**, 58-62.
Vonica, A. and Gumbiner, B. M. (2002). Zygotic Wnt activity is required for Brachyury expression in the early Xenopus laevis embryo. *Dev. Biol.* **250**, 112-127.
Wilson, P. and Keller, R. (1991). Cell rearrangement during gastrulation of Xenopus: direct observation of cultured explants. *Development* **112**, 289-300.
Winklbauer, R. (1988). Differential interaction of Xenopus embryonic cells with fibronectin in vitro. *Dev. Biol.* **130**, 175-183.
Winklbauer, R. and Schurfeld, M. (1999). Vegetal rotation, a new gastrulation movement involved in the internalization of the mesoderm and endoderm in Xenopus. *Development* **126**, 3703-3713.
Winning, R. S. and Sargent, T. D. (1994). Pagliaccio, a member of the Eph family of receptor tyrosine kinase genes, has localized expression in a subset of neural crest and neural tissues in Xenopus laevis embryos. *Mech. Dev.* **46**, 219-229.
Winning, R. S., Scales, J. B. and Sargent, T. D. (1996). Disruption of cell adhesion in Xenopus embryos by Pagliaccio, an Eph-class receptor tyrosine kinase. *Dev. Biol.* **179**, 309-319.
Winning, R. S., Wyman, T. L. and Walker, G. K. (2001). EphA4 activity causes cell shape change and a loss of cell polarity in Xenopus laevis embryos. *Differentiation* **68**, 126-132.
Winning, R. S., Ward, E. K., Scales, J. B. and Walker, G. K. (2002). EphA4 catalytic activity causes inhibition of RhoA GTPase in Xenopus laevis embryos. *Differentiation* **70**, 46-55.
Yin, C., Kiskowski, M., Pouille, P.-A., Farge, E. and Solnica-Krezel, L. (2008). Cooperation of polarized cell intercalations drives convergence and extension of presomitic mesoderm during zebrafish gastrulation. *J. Cell Biol.* **180**, 221-232.
Yokota, C., Kofron, M., Zuck, M., Houston, D. W., Isaacs, H., Asashima, M., Wylie, C. C. and Heasman, J. (2003). A novel role for a nodal-related protein; Xnr3 regulates convergent extension movements via the FGF receptor. *Development* **130**, 2199-2212.
Zhang, S.-C., Holland, N. D. and Holland, L. Z. (1997). Topographic changes in nascent and early mesoderm in amphioxus embryos studied by DiI labeling and by in situ hybridization for a Brachyury gene. *Dev. Genes Evol.* **206**, 532-535.

Legends to the Supplementary Figures

Figure S1. (A,B) Rescue of EphA4 knockdown (A4MO) by Xenopus EphA4 mRNA injection (A4) at indicated doses of MO or mRNA. Top: examples of sagittally fractures embryos at stage 11; bottom, archenteron lengths in experiments shown at top. (C,D) Kinase-dead EphA4 does not rescue and acts dominant-negatively. Top: examples of sagittally fractures embryos at stage 11; bottom, archenteron lengths in experiments shown at top. Asterisks, significant reduction.

Figure S2. Marker gene expression in control (A-E) and EphA4-MO embryos (F-J) at stage 11. (A,F) Gsc, prechordal mesoderm; (B,G) Cerberus, anterior mesendoderm; (C,H) Chordin, anterior chordamesoderm; (D,I) Xbra, chordamesoderm; (E,J) Sox2, neuroectoderm.

Figure S3. Control of Xbra expression. (A-D) Xbra expression under various treatments. A4MO, EphA4-MO; caMEK, constitutively active MEK; SU5402, inhibitor of FGF receptor; U0126, MAPK inhibitor; LY294002, PI3K inhibitor; DMSO, dimethylsulfoxide control.

Figure S4. Effect of Xbra injection on involution. (A) A4, EphA4-MO; Xbra, Xbra mRNA; doses as indicated. (B) Archenteron length in experiments shown in (A).

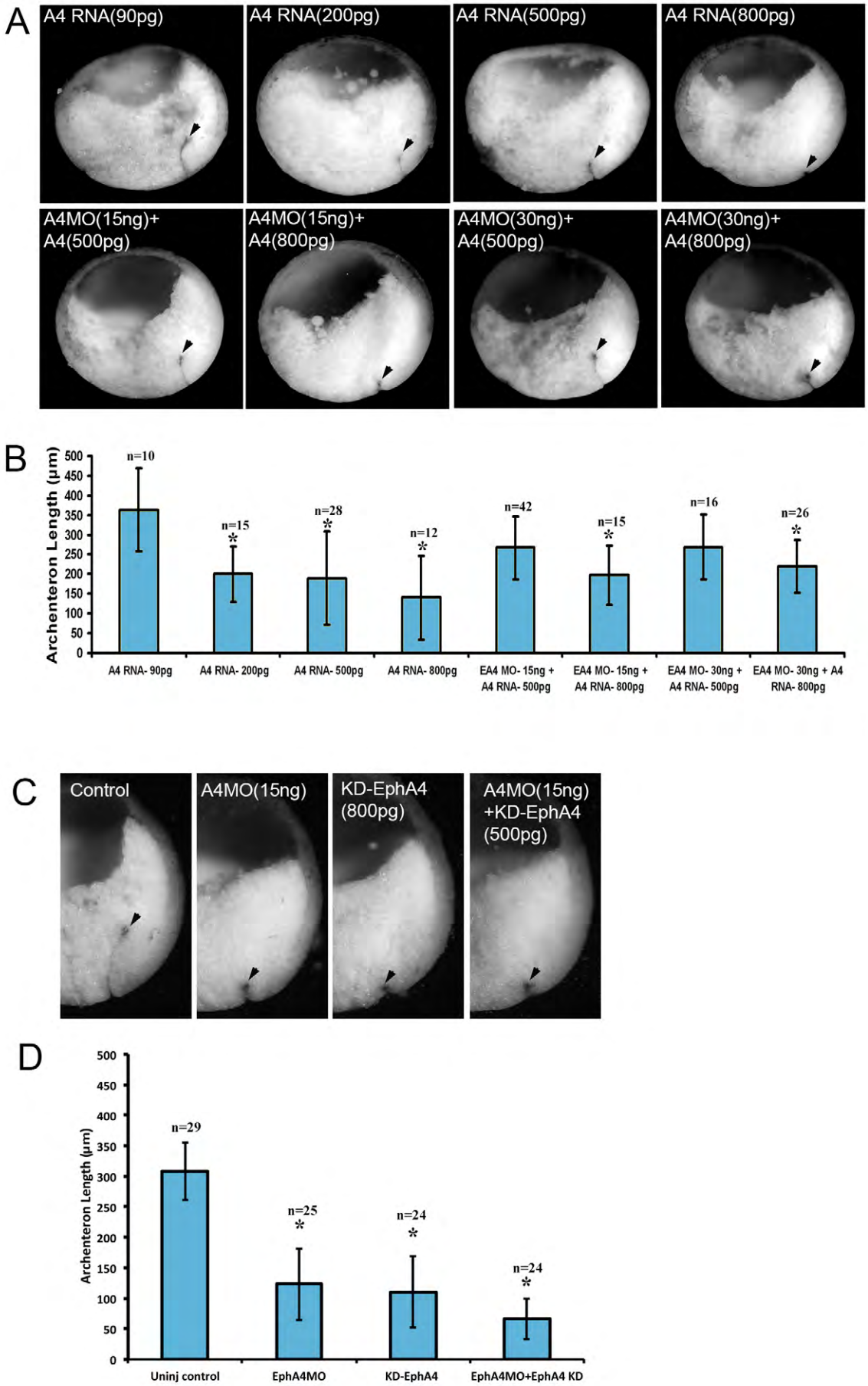
A
A4 RNA(90pg)
A4 RNA(200pg)
A4 RNA(500pg)
A4 RNA(800pg)
A4MO(15ng)+ A4(500pg)
A4MO(15ng)+ A4(800pg)
A4MO(30ng)+ A4(500pg)
A4MO(30ng)+ A4(800pg)
B
Archenteron Length (µm)
n=10
n=15
n=28
n=12
n=42
n=15
n=16
n=26
A4 RNA- 90pg
A4 RNA- 200pg
A4 RNA- 500pg
A4 RNA- 800pg
EA4 MO- 15ng + A4 RNA- 500pg
EA4 MO- 15ng + A4 RNA- 800pg
EA4 MO- 30ng + A4 RNA- 500pg
EA4 MO- 30ng + A4 RNA- 800pg
C
Control
A4MO(15ng)
KD-EphA4 (800pg)
A4MO(15ng) +KD-EphA4 (500pg)
D
Archenteron Length (µm)
n=29
n=25
n=24
n=24
Uninj control
EphA4MO
KD-EphA4
EphA4MO+EphA4 KD

Figure S1.

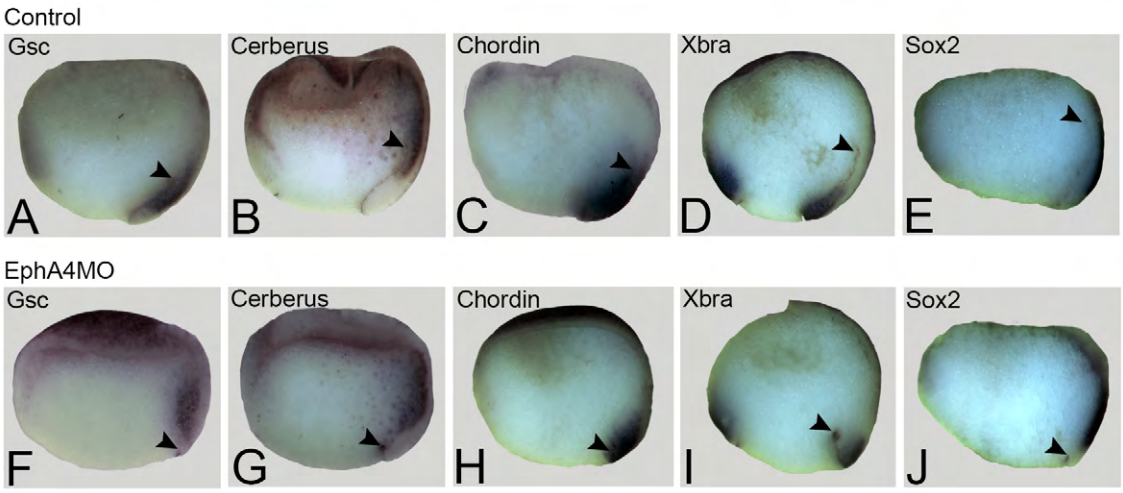
Control
Gsc
Cerberus
Chordin
Xbra
Sox2
A
B
C
D
E
EphA4MO
Gsc
Cerberus
Chordin
Xbra
Sox2
F
G
H
I
J

Figure S2.

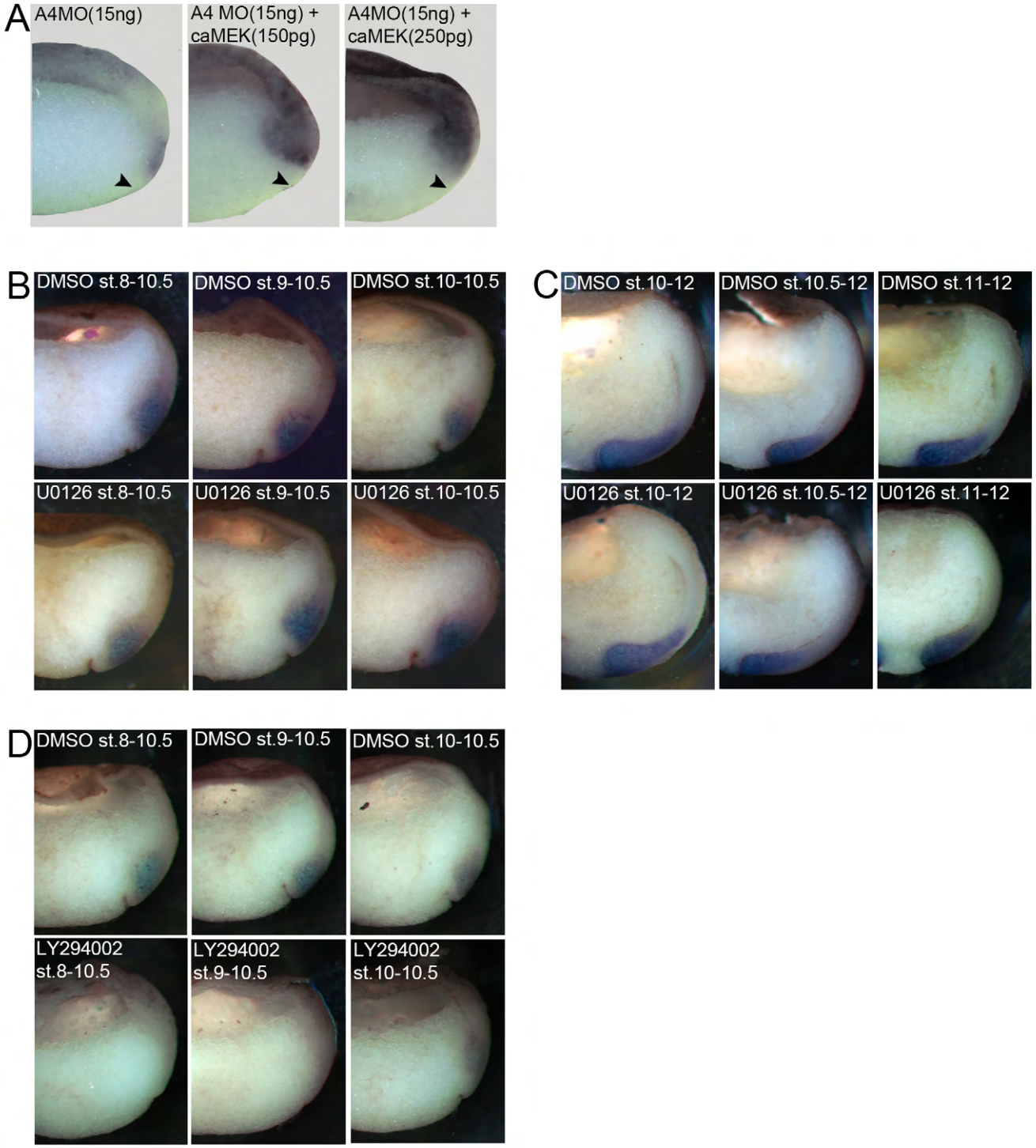
A
A4MO(15ng)
A4 MO(15ng) + caMEK(150pg)
A4MO(15ng) + caMEK(250pg)
B
DMSO st.8-10.5
DMSO st.9-10.5
DMSO st.10-10.5
U0126 st.8-10.5
U0126 st.9-10.5
U0126 st.10-10.5
C
DMSO st.10-12
DMSO st.10.5-12
DMSO st.11-12
U0126 st.10-12
U0126 st.10.5-12
U0126 st.11-12
D
DMSO st.8-10.5
DMSO st.9-10.5
DMSO st.10-10.5
LY294002 st.8-10.5
LY294002 st.9-10.5
LY294002 st.10-10.5

Figure S3.

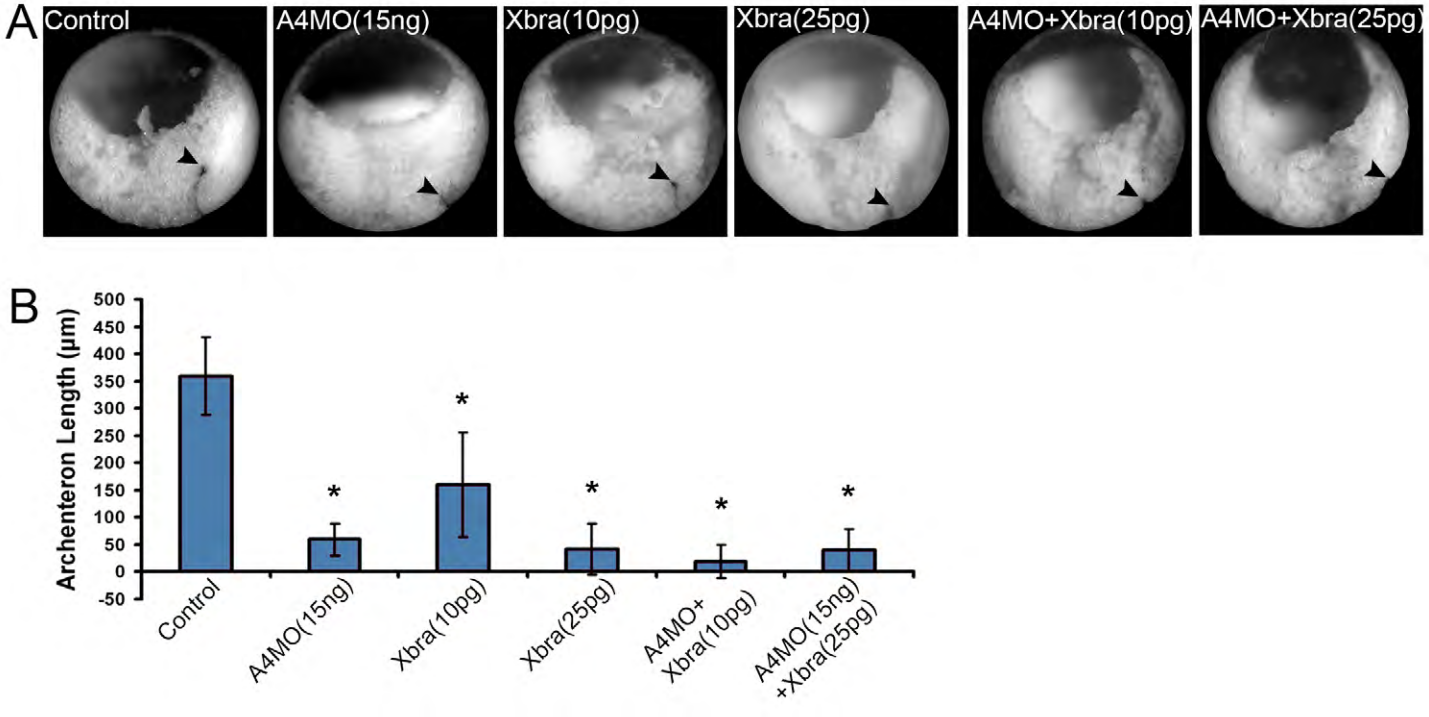
A
Control
A4MO(15ng)
Xbra(10pg)
Xbra(25pg)
A4MO+Xbra(10pg)
A4MO+Xbra(25pg)
B
Archenteron Length (µm)
500
450
400
350
300
250
200
150
100
50
0
-50
*
*
*
*
*
Control
A4MO(15ng)
Xbra(10pg)
Xbra(25pg)
A4MO+ Xbra(10pg)
A4MO(15ng) +Xbra(25pg)

Figure S4.

Movie titles and captions

Movie 1. Lip-BCR explant. Explant was made at stage 10+ and filmed for 2 hours. Ectodermal BCR (with darkly pigmented outer surface) is to the left, lip forms on the right. Inner surface is viewed.

Movie 2. Open-faced explant. Explant was made at stage 10+ and filmed for 45 min. Former vegetal side is to the left. For details see Fig. 3A.

Movie 3. Lip-only explant. Explant was made at stage 10.5 and filmed for 1 hour. Former vegetal side is to the left, cut surface is viewed. For details see Fig. 4E.

Movie 4. Explant of Xbra domain. Explant was made at stage 10.5 and filmed for 1 hour. Cut surface is viewed, as in movie 3. For details see Fig. 4H.

Movie 5. Explant of Xbra domain in side view. Stage 10.5 explant was filmed for 1 hour, viewed in 45° mirror submerged in culture buffer. For details see Fig.4I,J.

Movie 6. Lip-BCR explant expressing DN-Pak1. Explant was made at stage 10+ and filmed for 2 hours, as in movie 1, from embryo expressing DN-Pak1. Involution movement is compromised. Lip forms at the left, BCR is to the right.

Movie 7. Open-faced explants expressing DN-Pak1. Explant was made at stage 10+ from embryo expressing DN-Pak1 and filmed for 1 hour. For details see Fig. 8I.

Movie 1.

Movie 2.

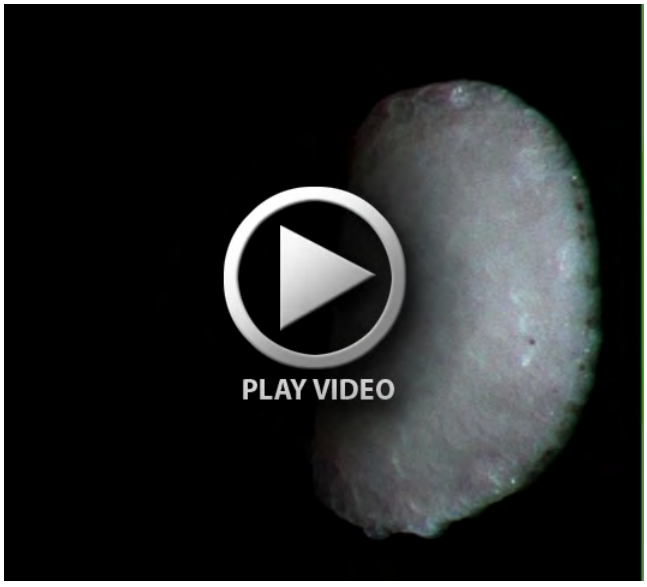

Movie 3.

Movie 4.

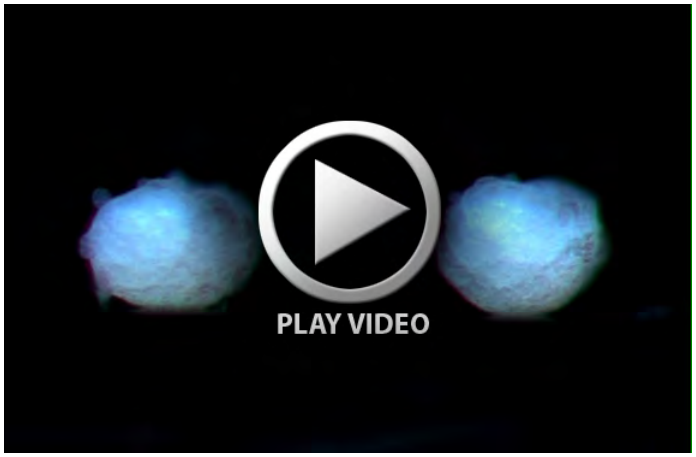

Movie 5.

Movie 6

Movie 7.